AD-777 038

DESIGN AND EVALUATION OF A HIGHLY SKEWED
PROPELLER FOR A CARGO SHIP

NAVAL SHIP RESEARCH AND DEVELOPMENT CENTER

FEBRUARY 1974

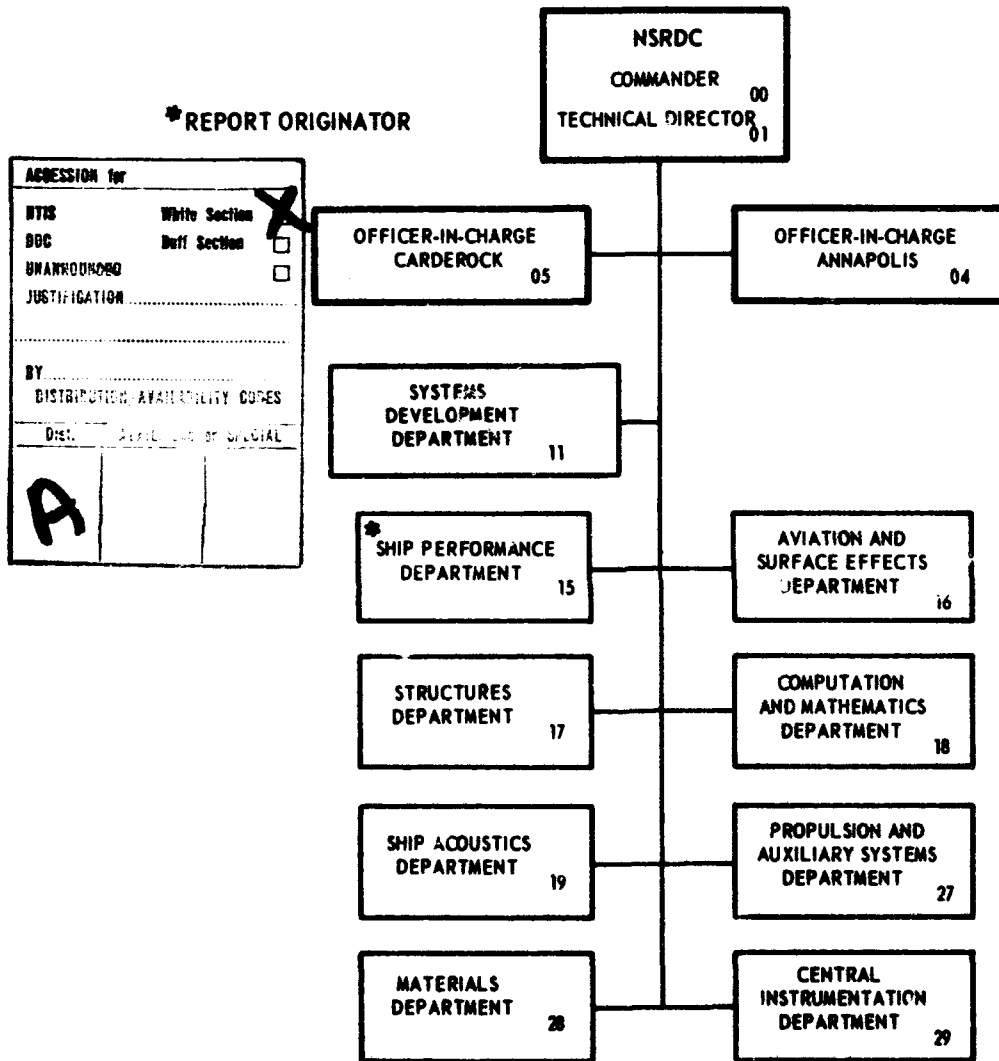The Naval Ship Research and Development Center is a U. S. Navy center for laboratory effort directed at achieving improved sea and air vehicles. It was formed in March 1967 by merging the David Taylor Model Basin at Carderock, Maryland with the Marine Engineering Laboratory at Annapolis, Maryland.

Naval Ship Research and Development Center

Bethesda, Md. 20034

MAJOR NSRDC ORGANIZATIONAL COMPONENTS

*REPORT ORIGINATOR

NSRDC
COMMANDER 00
TECHNICAL DIRECTOR 01

OFFICER-IN-CHARGE CARDEROCK 05	OFFICER-IN-CHARGE ANNAPOLIS 04

SYSTEMS DEVELOPMENT DEPARTMENT 11	
*SHIP PERFORMANCE DEPARTMENT 15	AVIATION AND SURFACE EFFECTS DEPARTMENT 16
STRUCTURES DEPARTMENT 17	COMPUTATION AND MATHEMATICS DEPARTMENT 18
SHIP ACOUSTICS DEPARTMENT 19	PROPULSION AND AUXILIARY SYSTEMS DEPARTMENT 27
MATERIALS DEPARTMENT 28	CENTRAL INSTRUMENTATION DEPARTMENT 29

AD 777038

DOCUMENT CONTROL DATA - R & D

Security classification of title, body of abstract and indexing annotation must be entered when the overall report is classified)

1 ORIGINATING ACTIVITY (Corporate author)	2a. REPORT SECURITY CLASSIFICATION
Naval Ship Research and Development Center Bethesda, Md. 20034	UNCLASSIFIED
	2b. GROUP

3 REPORT TITLE

DESIGN AND EVALUATION OF A HIGHLY SKEWED PROPELLER FOR A CARGO SHIP

4 DESCRIPTIVE NOTES (Type of report and inclusive dates)

Final Report

5 AUTHOR(S) (First name, middle initial, last name)

Robert J. Boswell and Geoffrey G. Cox

6 REPORT DATE	7a. TOTAL NO. OF PAGES	7b. NO OF REFS
February 1974	58	43
8a. CONTRACT OR GRANT NO	9a. ORIGINATOR'S REPORT NUMBER(S)	
b. PROJECT NO	3672	
c. NSRDC Work Unit 1544-051 NSRDC Work Unit 1544-057	9b OTHER REPORT NO(S) (Any other numbers that may be assigned this report)	
d.		

10 DISTRIBUTION STATEMENT

Approved for Public Release: Distribution Unlimited

11 SUPPLEMENTARY NOTES	12 SPONSORING MILITARY ACTIVITY

13 ABSTRACT

The design process and model evaluation of a highly-skewed propeller for a modern cargo ship are given. The design process is discussed in detail, including considerations of cavitation, mean and fatigue strength, and propeller-excited vibratory forces. Model experimental results are presented which tend to confirm the design process and to show that the highly skewed propeller possesses propulsion performance comparable to the propeller now fitted to the ship, delays the inception of cavitation by 2 knots, has less tendency towards cavitation erosion than the fitted propeller, and possesses adequate strength for ahead and steady astern operation. Calculations, using unsteady lifting-surface theory, indicate that the highly skewed propeller will reduce blade-frequency thrust and torque by 90 percent, will reduce blade-frequency transverse horizontal bearing force by 60 percent, and will increase blade-frequency vertical bearing force by 2 percent, compared to the propeller currently installed on the ship.

14 KEY WORDS	LINK A		LINK B		LINK C	
	ROLE	WT	ROLE	WT	ROLE	WT
Propeller						
Skewed Propeller						
Marine Propeller						
Strength						
Vibration						
Model Evaluation						
Cargo Ship						
Propulsion						
Cavitation						
Unsteady Loading						

DEPARTMENT OF THE NAVY

NAVAL SHIP RESEARCH AND DEVELOPMENT CENTER

BETHESDA, MARYLAND 20034

DESIGN AND EVALUATION OF A HIGHLY SKEWED

PROPELLER FOR A CARGO SHIP

by

Robert J. Boswell and Geoffrey G. Cox

APPROVED FOR PUBLIC RELEASE: DISTRIBUTION UNLIMITED

February 1974

Report 3672

TABLE OF CONTENTS

Page

LIST OF FIGURES

ii

LIST OF TABLES

iii

NOTATION

A_e	Expanded area $Z \int_{r_h}^{R} c\,dr$
A_0	Disk area of propeller πR^2
C_L	Lift coefficient of section at ideal angle of attack $L/(\tfrac{1}{2}\rho V_r^2)$
C_{Th}	Thrust-loading coefficient $T/(\tfrac{1}{2}\rho A_0 V_A^2)$
c	Section chordlength
D	Propeller diameter
E	Modulus of elasticity
EAR	Expanded-area ratio A_E/A_0
f_M	Section camber
G	Nondimensional circulation $\Gamma/\pi DV$
g	Acceleration due to gravity
H	Hydrostatic head at local position minus vapor head
J	Advance coefficient V_A/nD
k_c	Camber correction factor
n	Propeller revolutions per unit time
$(P/D)_I$	Propeller section hydrodynamic pitch ratio $\pi x \tan\beta_I$
P	Propeller section pitch
P_D	Delivered power at propeller $2\pi nQ$
P_E	Effective power RV
Q	Propeller torque
q	Harmonic of wake
R	Propeller radius; resistance of ship
R_n	Reynolds number $c_{0.7}\,V_{r_{0.7}}/\nu$
r	Radial distance
r_h	Radius of hub
T	Propeller thrust
t	Thrust deduction fraction $t = (T-R)/T$; or blade section maximum thickness
V_A	Speed of advance of propeller $V(1-w_T)$
V	Ship Speed
V_r	Resultant inflow velocity to blade section

w_T	Taylor wake fraction determined from thrust identity
w_x	Local wake fraction
x	Nondimensional radial distance r/R
Z	Number of blades
β	Circumferential mean advance angle $\tan^{-1}[V(1-w_x)/\pi x n D]$
β_I	Hydrodynamic flow angle
Γ	Circulation about blade section
$\Delta\alpha$	Deviation from section ideal angle of attack in two-dimensional flow
$\Delta\beta$	Local advance angle minus circumferential mean advance angle
η_B	Propeller behind efficiency TV_A/P_D
η_D	Propulsive efficiency P_E/P_D
θ_S	Projected skew angle
ν	Kinematic viscosity of water
ρ	Mass density of water
σ	Cavitation number at shaft centerline, based on speed of advance $2gH/V_A^2$
σ_r	Local cavitation number $2gH/V_r^2$

ABSTRACT

The design process and model evaluation of a highly-skewed propeller for a modern cargo ship are given. The design process is discussed in detail, including considerations of cavitation, mean and fatigue strength, and propeller-excited vibratory forces. Model experimental results are presented which tend to confirm the design process and to show that the highly skewed propeller possesses propulsion performance comparable to the propeller now fitted to the ship, delays the inception of cavitation by 2 knots, has less tendency towards cavitation erosion than the fitted propeller, and possesses adequate strength for ahead and steady astern operation. Calculations, using unsteady lifting-surface theory, indicate that the highly skewed propeller will reduce blade-frequency thrust and torque by 90 percent, will reduce blade-frequency transverse horizontal bearing force by 60 percent, and will increase blade-frequency vertical bearing force by 2 percent, compared to the propeller currently installed on the ship.

ADMINISTRATIVE INFORMATION

INTRODUCTION

The procedure for designing propellers in current use at the Naval Ship Research and Development Center (the Center), including a summary of the analytical techniques, computational procedures, and critical design judgments was published recently.[1] Another recently published paper[2] presented extensive theoretical and experimental data that demonstrated the potentially substantial advantages of highly skewed propellers, compared to propellers with either moderate or no skew. These advantages include substantial reductions in unsteady propeller bearing forces and moments due to operation in a nonuniform flow field,[3]

---

[1]Cox, G.G. and W.B. Morgan, "The Use of Theory in Propeller Design," Marine Technology, Vol. 9, No. 4, pp. 419–429 (Oct 1972). A complete listing of references is on page(s) 49 through 51.

[2]Cumming, R.A., W.B. Morgan and R.J. Boswell, "Highly Skewed Propellers," Transactions of the Society of Naval Architects and Marine Engineers, Vol. 80 (1972).

[3]Boswell, R.J. and M.L. Miller, "Unsteady Propeller Loading- Measurement, Correlation with Theory, and Parametric Study," NSRDC Report 2625 (Oct 1968).

reduction in propeller-induced vibratory pressures,[4] and improved tolerance to inception of cavitation caused by fluctuations in angle of attack due to operation in a wake.[5,6,7]

These benefits can be achieved without adverse effects on ahead efficiency, without adverse effects on thrust breakdown due to cavitation, and with only minor decrease in backing efficiency.[6] Although strength characteristics of highly skewed propellers are substantially more complicated than for conventional propellers, there is apparently no problem in ensuring strength integrity of highly skewed propellers.[2]

The major purpose of the present report is to describe an application of the propeller-design procedure in use at the Center for a case presenting severe vibration and cavitation problems and to demonstrate the techniques for incorporating high skew into the design to help alleviate these problems. Model experimental results are presented to substantiate the design techniques and design decisions, considering propulsion, cavitation, cavitation erosion, and strength.

The application presented is for a modern single-screw cargo ship; see Figure 1. With its currently fitted propeller this ship experiences severe propeller-induced vibration and substantial cavitation erosion on the propeller. These problems are, to a large measure, a result of the severe circumferential variation of the wake in the propeller disk; see Figures 2 and 3. The primary objective of designing a highly skewed propeller for this ship is to reduce the propeller-induced vibration excitation forces. The secondary objective is to lessen the cavitation-erosion problem.

PROPELLER DESIGN PROCEDURE

The propeller was designed to absorb 30,000 horsepower at the specified conditions of displacement, t... and hull conditions. Resistance and propulsion data were obtained from the appropriate experiments on the model hull, fitted for propulsion experiments with a model of the propeller currently installed on the vessel. These data indicated that the ship should have a speed of approximately 24.5 knots when absorbing 30,000 horsepower at design conditions.

[4]Teel, S.S. and S.B. Denny, "Field Point Pressures in the Vicinity of a Series of Skewed Marine Propellers," NSRDC Report 3278 (Aug 1970).

[5]Denny, S.B., "Cavitation and Open-Water Performance of a Series of Propellers Designed by Lifting-Surface Methods," NSRDC Report 2878 (Sep 1968).

[6]Boswell, R.J., "Design, Cavitation Performance, and Open Water Performance of a Series of Research Skewed Propellers," NSRDC Report 3339 (Mar 1971).

[7]Boswell, R.J., "The Effect of Skew on Cavitation of Marine Propellers," presented at the American Society of Mechanical Engineers Cavitation Forum, Pittsburgh, Pa. (Jun 1971).

Basically, the propeller was designed in five phases.

1. Preliminary Design: Preliminary design analysis was conducted, using lifting-line calculations,[8,9] to determine the parameters for which the propeller was to be designed so that the propeller would be compatible with the ship, installed propulsion machinery, and transmission from the standpoint of efficiency and vibration.

2. Radial Distribution of Loading: Desired radial distribution of loading was determined, using lifting-line calculations. The theory is for inviscid flow; however, viscous drag was suitably taken into account by a strip-theory analysis.

3. Skew: Magnitude and distribution of skew were selected from considerations of cavitation and propeller-induced, vibration excitation. Calculations were performed, using unsteady lifting-surface theory and the estimated wake[10] to minimize the pertinent components of unsteady bearing forces.

4. Blade Width and Thickness: Blade shape, area, and thickness distribution were determined from the standpoint of cavitation and strength. Cavitation erosion and thrust breakdown should not occur at the design conditions.

5. Final Geometry: The final camber and pitch distributions were determined, using lifting-surface calculations. A strength check was performed on the final blade configuration.

These phases have been specified as a guide to the major steps in the designing process. However, most of the steps are closely interrelated, and iterations between the steps were necessary. These will be discussed in detail in the following sections.

PRELIMINARY DESIGN

In the preliminary design, the major propeller parameters, such as diameter, number of blades, and rotational speed, were determined so that the propeller would be compatible with the ship, installed propulsion machinery, and transmission from considerations of vibration and efficiency. The maximum diameter was limited by the geometry of the aperture and the propeller-induced unsteady pressure forces on the hull. These pressure forces decreased with increasing tip clearance.[4] For the application considered here, a minimum tip clearance of 12 percent of the propeller diameter 0.12 D was selected. This limited the maximum allowable propeller diameter to 23 feet. The rotational speed and number of blades was specified so that the blade-rate frequency would be sufficiently different from any resonant frequency of the hull, shafting, or propulsion machinery. These considerations dictated six blades and a

---

[8]Lerbs, H.W., "Moderately Loaded Propellers with a Finite Number of Blades and an Arbitrary Distribution of Circulation," Transactions of Society of Naval Architects and Marine Engineers, Vol. 60, pp. 73–117 (1952).

[9]Morgan, W.B. and J.W. Wrench, "Some Computational Aspects of Propeller Design," Methods of Computational Physics, Vol. 4, Academic Press, Inc., New York (1965) pp. 301–331.

[10]Hadler, J.B. and H.M. Cheng,."Analysis of Experimental Wake Data in Way of Propeller Plane of Single and Twin-Screw Ship Models," Transactions of Society of Naval Architects and Marine Engineers, Vol. 73, pp. 287–414 (1965).

rotational speed of 107 rpm. If resonance excitation were not a problem, then the number of blades would have been selected, based upon an analysis of the harmonic distribution of the wake velocity, to minimize the most important components of the bearing forces. This would involve a tradeoff with skew as discussed in the section on skew.

From considerations of efficiency, the major propeller parameters were selected by lifting-line[8,9] calculations for a pertinent series of propellers operating in the spatially varying velocity field. Using lifting-line methods is superior to using design charts derived from propulsion experiments of systematic series of propellers in uniform flow, since wake distribution is not considered in series data. Therefore, use of design charts can lead to a propeller which may not be the most effective. For the application considered in this report, the best propeller diameter from efficiency considerations is greater than the maximum allowable diameter of 23 ft, based on vibration. Further, considerations of vibration dictated the number of blades and severely restricted the allowable range of rotational speed. Therefore, from the preliminary design the following were selected

Diameter D	23 feet
Number of Blades Z	6
Rotational Speed	107 rpm

RADIAL DISTRIBUTION OF LOADING

Next, the radial distribution of loading was investigated, using lifting-line methods based on the Lerbs induction factors.[8,9] For this design it was desirable to unload the blade tip to help alleviate the tendency toward cavitation erosion in the vicinity of the tip. It has been demonstrated that cavitation erosion is a problem of the propeller currently installed on the ship. Unloading the blade tip also tends to delay inception of tip-vortex cavitation which can cause erosion on the rudder, to reduce blade-frequency pressures on the hull above the propeller, and to reduce blade-stress level. The disadvantage of unloading the tip is that there is a small reduction in propeller efficiency which leads to a small reduction in ship speed at a given delivered power.

Five hydrodynamic pitch-ratio distributions $(P/D)_1$ were investigated (Figure 4) with corresponding circulation distributions G; see Figure 5. The Lerbs optimum pitch distribution and the pitch distribution with mathematically unloaded root and tip were investigated to serve as guides in selecting the degree of tip unloading. Lerbs optimum is an estimate of the hydrodynamic pitch distribution which would produce the highest efficiency for a wake-adapted propeller.[8] This would be a logical choice for an application in which there were no cavitation or vibration problems.

4

Three pitch distributions were investigated, designated Types I, II, and III, which would unload the tip by varying degrees. All three followed the Lerbs optimum formulation from the root to the 60-percent radius. The greater the tip unloading was, the greater the potential improvement was in back bubble cavitation near the tip, tip vortex cavitation, vibration, and strength; however, the greater the reduction was in ship speed at design delivered power. Extreme reduction in tip loading could tend to aggravate the leading-edge sheet cavitation because of variation in angle of attack near the tip. Table 1 shows the speed predicted by the lifting-line theory at design delivered power P_D = 30,000 horsepower for the various load distributions for expanded-area ratio EAR = 0.77. Load distribution Type I was selected, representing a calculated sacrifice in ship speed at design delivered power of 0.14 knots, compared to the Lerbs optimum distribution.

SKEW

Next, magnitude and distribution of skew were selected. Available data[2] indicate that a substantial amount of properly applied skew significantly reduces the magnitude of propeller-induced, vibration-excitation forces transmitted through the shafting to the bearings and through the water to the hull plating and increases the tolerance to cavitation inception due to operation in a circumferentially varying flow field. Although these data generally show that skew at the blade tip of as much as blade spacing, $2\pi/Z$* is generally desirable, they provide little guidance to the proper tip skew and radial distribution of skew that should be applied for a given application.

For the design application considered in this report, skew may be beneficial from considerations of cavitation. The severe circumferential variation of the wake (Figure 2) suggests that leading-edge sheet cavitation arising from variation in angle of attack is likely to be a serious problem. Skew tends to increase the tolerance to angle of attack before the inception of leading-edge sheet cavitation.[6] Although the mechanism of this phenomenon is not fully understood, it is primarily dependent upon the angle of sweep of the blade leading edge t the local resultant inflow velocity. Sharp changes in leading-edge curvature are to be avoided since such changes may reduce the cavitation inception speed. Therefore, from considerations of cavitation, the radial distribution of skew and chordlengths should be selected to produce a smooth, highly swept leading edge.

For appraising propeller-induced vibration, the total vibration-excitation force—the vector sum of pressure-force and bearing-force components—must be considered. This, of course, requires a knowledge of the relative phase of the pressure forces to the bearing forces. Only limited indirect and inconclusive experimental data are available concerning the relative phases

---

*For this amount of skew, the tip of each blade lies along the same radial line as the midchord of the section at the root of the following blade.

5

TABLE 1 – EFFECT OF RADIAL LOAD DISTRIBITON ON PROPULSION PERFORMANCE

	V in Knots at P_D = 30,000 HP	P_D at V = 24.36 Knots	η_B at V = 24.36 Knots
Lerbs Optimum	24.50	29,325	0.695
Tip and Root Unloaded	24.34	30,190	0.664
Tip Unloaded, Type I	24.36	30,000	0.672
Tip Unloaded, Type II	24.37	29,881	0.676
Tip Unloaded, Type III	24.38	29,782	0.680

of pressure-force to bearing-force components behind hulls of the kind considered in this report.[11] These data neglect the influence of cavitation, which significantly influences amplitude and phase of the pressure forces.[12,13,14] Furthermore, no theory is available by which the amplitude and phase can be accurately calculated for pressure forces on a hull having a complex geometry and wake pattern, such as the hull considered in this report. Therefore, it is beyond the present state of the art to determine precisely the magnitude and distribution of skew that will minimize the total, pressure plus bearing, vibration-excitation force in a specified direction. However, a skew can be specified which will substantially reduce the amplitude of both pressure force and bearing-force components.

Experimental measurements of the propeller-induced pressures on a flat plate show that the blade-frequency amplitude of the propeller-induced pressure monotonically decreases with increasing skew. This holds true for operations in both uniform and circumferentially varying flow fields.[4] These data suggest that for reducing propeller-induced, vibration-excitation forces due to unsteady pressures on the hull, the projected skew angle at the blade tip should be approximately the angular spacing between the blades, $2\pi/Z$.

For unsteady bearing forces, the radial distribution of skew is of first order importance, since cancellation of the unsteady loading on the blades from root to tip is the mechanism by which skew reduces the unsteady bearing forces. The effect of radial distribution of skew on bearing forces can be evaluated by using unsteady lifting-surface theory.[15] The validity of this theory has been substantiated by excellent agreement with experimental results[3] obtained for a series of propellers operating in simplified wake patterns generated by upstream screens. The accuracy of calculations made by this theory may not be as good when the propeller is operating in the wake of the hull because the propeller may influence the wake, and the harmonic content of the wake is much more complex. However, in view of the agreement obtained between theory and experiment for the simplified wakes, the theory was used to investigate the effect of the magnitude and distribution of skew on the unsteady bearing forces that might be produced by a propeller operating in the wake of the ship being considered in this report.

---

[11]Lewis, F.M., "Propeller Vibration Forces in Single Screw Ships," Transactions of Society of Naval Architects and Marine Engineers, Vol. 77, pp. 318–343 (1969).

[12]Denny, S.B., "Comparisons of Experimentally Determined and Theoretically Predicted Pressures in the Vicinity of a Marine Propeller," David Taylor Model Basin Report 2349 (May 1967).

[13]Van Oossanen, P. and J. van dir Kouy, "Vibratory Hull Forces Induced by Cavitating Propellers," presented at the Spring Meeting of the Royal Institution of Naval Architects, London, England (Apr 1972).

[14]Huse, E., "Pressure Fluctuations on the Hull Induced by Cavitating Propellers," Norwegian Ship Model Experimental Tank Publication 111 (Mar 1972).

[15]Tsakonas, S. and W.R. Jacobs, "Propeller Loading Distributions," Journal of Ship Research, Vol. 13, No. 4, pp. 237–256 (Dec 1969).

Calculations were performed to evaluate the effect of skew and number of blades on the blade-frequency amplitude of the thrust, torque, vertical force, and transverse horizontal force on the propeller. Hull resonance characteristics dictated that a six-bladed propeller be selected for the design considered in this report; however, calculations for different numbers of blades have been presented to illustrate the interrelation between skew and number of blades. All geometric parameters were the same as those of the final highly skewed propeller design—except skew, number of blades, and blade width, which was adjusted so that expanded-area ratio would be constant independent of the number of blades. Calculations were made for four-, five-, six- and seven-bladed propellers with projected skew angle at the blade tip equal to 0, 0.5, and 1.0 times angular spacing of the blades, $2\pi/Z$. For all cases, the skew has been distributed linearly from root to tip, $d\theta_s/dr$ = constant.

These results demonstrate that skew has a first order effect on the various components of unsteady bearing force; see Figure 6. They further demonstrate the complex nature of the effect of skew on the various components of bearing force. The trends shown in Figure 6 can be qualitatively explained by inspection of the pertinent harmonics of the wake. The pertinent odd harmonics of the wake q = 3, 5, and 7 change sign with increasing radius; however, the even harmonics q = 4, 6, and 8 do not change sign. This change of sign of the odd harmonics is typical of single-screw merchant ships.[10] The blade-frequency thrust and torque are caused by the Zth harmonic of the wake, where Z is the number of blades, whereas the blade frequency vertical force and transverse horizontal force are each produced by a combination of the Z + 1 and Z − 1 harmonics of the wake. For an unskewed blade, a wake harmonic which changes sign with radius results in some cancellation from root to tip of the same harmonic of unsteady loading on the blade; therefore, for the Z − 1, Z and Z + 1 harmonics, the tendency is to reduce the associated component of blade-frequency loading. Therefore, for unskewed or low-skewed propellers an odd number of blades tends to produce lower blade-frequency thrust and torque than does an even number of blades; whereas, an even number of blades tends to produce lower blade-frequency vertical force and transverse horizontal force than does an odd number of blades. The response of the propeller to the wake is complex; therefore, simplified analysis of the wake should be used only as an initial guide, especially for the vertical and transverse horizontal forces which respond simultaneously to two harmonics of the wake. The results shown in Figure 6 confirm that for the unskewed propellers, an odd number of blades produces a lower blade-frequency thrust and torque, and an even number of blades, generally, but not always, produces lower blade frequency vertical and transverse horizontal forces.

Introduction of high skew further complicates the analysis. High skew introduces a gradual phase shift with increasing radial position of the blade relative to the wake, somewhat analogous to the more sudden phase shift of the odd harmonic of the wake relative to an

8

unskewed blade. Therefore high skew tends to be most effective in reducing the blade-frequency components which are largest for unskewed propellers, i.e., thrust and torque for even-bladed propellers, and vertical and transverse horizontal side forces for odd-bladed propellers. For all cases like those shown in Figure 6, linear skew equal to blade spacing reduces the pertinent component by a minimum of 80 percent from the value for the corresponding unskewed propeller. Skew may be less effective for reducing thrust and torque for odd-bladed propellers, and side forces for even-bladed propellers, which tend to be smaller for unskewed propellers by virtue of the phase shift with increasing radius of the odd harmonics of the wake. Figure 6, which corresponds to a linear variation of skew with radius $d\theta_s/dr =$ constant, shows that in certain instances these components of blade-frequency loading can be increased slightly by skew. However, by properly specifying the distribution of skew with radius, any specified component of unsteady loading can be reduced to a small fraction of its value for an unskewed propeller. In principle, it can be reduced to zero. *Figure 6 further demonstrates that when high skew is used, the criterion of minimizing the unsteady bearing forces may dictate a different number of blades than for the case in which high skew is not utilized.*

To minimize a specified component of unsteady loading, the radial distribution of skew must be carefully matched to the amplitude and phase of the pertinent harmonics of the wake to secure maximum cancellation from root to tip.[2,16,17] The optimum distribution is, in general, different for the different components of unsteady loading. For the design considered in this paper, resonances dictated that six blades be used, and from considerations of blade-frequency pressure forces and cavitation, the maximum skew at the blade tip was selected to be blade angular spacing of $2\pi/6$ radians = 60 degrees. For six blades and 60 degrees skew, the effect of radial distribution of skew on blade-frequency bearing forces was investigated. Four distributions have been explored; see Figure 7:

1. Linear, in which $(d\theta_s/dr)$ = constant.
2. One in which most of the skew is concentrated near the blade tip.
3. One intended to reduce the blade-frequency thrust and torque below the respective values for the linear distribution. This distribution has negative skew from the 20- to the 40-percent radii and is linear from the 40-percent radius to the tip.
4. One that attempts to reduce the blade-frequency vertical and transverse horizontal forces below the respective values for the linear distribution. This distribution is characterized by a large slope $d\theta_s/dr$ between the 40- and 80-percent radii where the fifth and seventh

[16]Breslin, J.P., Discussion of paper, "Highly-Skewed Propellers," by Cumming, Morgan, and Boswell, Transactions of Society of Naval Architects and Marine Engineers, Vol. 80 (1972).

[17]Brown, N.A., Discussion of paper, "Highly-Skewed Propellers," by Cumming, Morgan, and Boswell, Transactions of Society of Naval Architects and Marine Engineers, Vol. 80 (1972).

harmonics of the wake are large and do not change sign. Near the tip where fifth and seventh harmonics of the wake change sign, $d\theta_s/dr$ is zero.

The blade-frequency thrust, torque, vertical side force, and horizontal side force for these four distributions and the corresponding unskewed propeller are presented in Figure 8. These results show that:

1. Distribution (1) is quite effective in reducing blade-frequency thrust, torque, and horizontal force; however, it does not reduce the vertical force below that of the unskewed propeller.

2. Distribution (2) is not nearly as good as distribution (1) for reducing any of the blade frequency components. Too much skew is concentrated near the tip where the amplitude of the sixth harmonic of the wake is small, and where the fifth and seventh harmonics of the wake change sign.

3. Distribution (3) is slightly better than the linear distribution in reducing all of the blade-frequency components. The disadvantage of this distribution is the shape of the blade resulting from the negative skew at the inner radii. This may produce higher stress levels than will distribution (1).

4. Distribution (4) substantially reduces the blade-frequency vertical and horizontal side forces relative to distribution (1) at the expense of somewhat larger blade-frequency thrust and torque. However, all components are less than 25 percent of their respective values for the unskewed propeller. The disadvantage of this distribution is the resulting shape of the blade near the tip. This shape may adversely affect the cavitation performance.

Distribution (2) was not very effective for reducing bearing forces, distribution (3) had a potentially adverse effect on strength, and distribution (4) had a potentially adverse effect on cavitation. Therefore, distribution (1) was selected for use in the design under consideration in this paper. This linear distribution of skew, together with a mathematical blade outline, will yield a smooth leading-edge curvature for cavitation criteria, will produce a substantial reduction in vibration-excitation from both unsteady bearing forces and pressure forces, and with proper selection of blade thickness will provide adequate strength.

For comparison, the bearing forces were calculated for the propeller currently fitted to the ship; see Figure 9. These results indicated that the highly skewed propeller reduced blade-frequency thrust and torque by 90 percent, reduced blade-frequency transverse horizontal force by 60 percent, and increased blade-frequency transverse vertical force by 2 percent, relative to the propeller currently installed on the ship.

BLADE WIDTH AND THICKNESS

Next, the detailed blade geometry was selected, that is, expanded-area ratio (EAR) and radial distribution of chordlength and thickness. Each of these were carefully selected so

10

that the blade possessed adequate strength and minimum tendency towards cavitation erosion. In addition, propeller efficiency could not be materially sacrificed.

Data for merchant ship propellers[18] indicated that the design described here must have a minimum expanded-area ratio of 0.75 to avoid thrust breakdown at full power. Greater blade width generally increases strength but reduces speed at a specified delivered power because of increased viscous drag. Lifting-line and strip-theory calculations showed that increasing expanded-area ratio by 0.02 reduced the calculated ship speed at design power by 0.02 knots. Based on these considerations, an expanded-area ratio of 0.77 was selected.

To pick the best blade shape for cavitation performance, it would have been preferable to calculate the cavitation phenomena in nonuniform flow. However, unsteady lifting-surface theory for propellers is not yet sufficiently developed to predict cavitation phenomena. Therefore, for design purposes the cavitation inception was estimated by calculating the angle of attack variation by simplified quasi-steady theory[19] and by estimating the resultant pressure distribution on the blade sections by two-dimensional potential flow theory.

The range of advance angle $\beta + \Delta\beta_{max}$ to $\beta - \Delta\beta_{max}$ and cavitation number σ_r experienced by each blade section during one revolution was calculated directly from the wake data.[10] From the variation in advance angle, an estimate of the variation in effective angle of attack of each blade section was made by simplified quasi-steady theory, based upon elliptic loading of wings of finite-aspect ratio.[19]

$$\Delta\alpha = \frac{-\Delta\beta}{k_c + (2/A_e)}$$

where $A_e = C_i /(\pi \tan(\beta_I - \beta))$ is the effective aspect ratio, and k_c is the ratio of camber required to produce the lift coefficient at ideal angle of attack on the propeller blade to camber required to produce the same lift coefficient at the ideal angle of attack in two-dimensional flow. For these preliminary cavitation considerations, k_c can be suitably obtained from either References 2, 20, 21, or 22.

---

[18]Burrill, L.C. and A. Emerson, "Propeller Cavitation: Further Tests on 16-Inch Model Propellers in the Kings College Cavitation Tunnel," North East Coast Institution of Engineers and Shipbuilders, Vol. 79, pp. 295–320 (1962–63).

[19]Rader, H.P., "Cavitation Phenomena in Nonuniform Flows," Appendix 2 of the Cavitation Committee Report, Proceedings of the 12th International Towing Tank Conference, Rome, Italy, pp. 351–364 (Sep 1969).

[20]Morgan, W.B., V. Silovic and S.B. Denny, "Propeller Lifting Surface Corrections," Transactions of Society of Naval Architects and Marine Engineers, Vol. 76, pp. 309–347 (1968).

[21]Cox, G.G., "Corrections to the Camber of Constant Pitch Propellers," Transactions of Royal Institute of Naval Architects, Vol. 103, pp. 227–243 (1961).

[22]Minaas, K. and O.H. Slaattelid, "Lifting Surface Corrections for 3-Bladed Optimum Propellers," International Shipbuilding Progress, Vol. 18, No. 208, pp. 437–452 (Dec 1971).

11

The inception of cavitation was then predicted by entering cavitation inception diagrams derived from potential flow theory for two-dimensional sections of prescribed thickness and meanline distributions.[23] The NACA (National Advisory Committee for Aeronautics) 66 (Center modified)[23] thickness form and the NACA a = 0.8 meanline were used in the design described in this report. The propeller was designed so that the blade section at each radius would operate at ideal angle of attack at the circumferential mean advance velocity. Figure 10 shows an example of such cavitation diagrams or buckets—the solid lines are the buckets—for a range of angles of attack versus local cavitation number σ_t with the thickness-to-chordlength ratio t/c as a parameter. A set of such diagrams was used, each diagram representing a different camber-to-chord ratio f_M/c. The inside of the buckets are cavitation-free regions with the top and bottom of the buckets indicating leading-edge suction-side, back, and pressure-side, face, cavitation, respectively. The steep portion of the buckets indicates inception of back bubble cavitation. A study of these curves will immediately reveal a tradeoff choice, namely, by selection of thickness-to-chord ratio, it is often possible to achieve increased latitude against leading-edge cavitation due to fluctuating angle of attack at the price of earlier inception of back bubble cavitation at ideal angle of attack.

The dashed lines in Figure 10 show the approximate range of operating conditions for blade sections operating in the wake of this ship. In practice a different set of cavitation buckets may be used for each radius, the suitable set being the one having the camber required to produce the specified lift coefficient in two-dimensional flow. The operating conditions are primarily a function of the wake distribution and the ship speed; the only propeller parameters that significantly influence these curves are diameter and rpm. From Figure 10 it is apparent that it is not possible to avoid cavitation in the region from the blade tip to the 50-percent radius. This situation is a direct result of the severe circumferential nonuniformity of the flow into the propeller disk.

The blade-section t/c can be selected based on the cavitation buckets[23] by one of several criteria, for instance,

1. To avoid leading-edge sheet cavitation; however, this would result in excessively high values of t/c from consideration of back bubble cavitation and strength in the vicinity from the 50-percent radius to the tip. Such a blade would suffer severe back bubble cavitation in this region.

2. To provide a maximum factor of safety for back bubble cavitation. This dictates a very low value of t/c. The minimum allowable thickness would be dictated by strength

[23]Brockett, T., "Minimum Pressure Envelopes for Modified NACA Sections with NACA a = 0.8 Camber and BUSHIPS Type I and Type II Sections," David Taylor Model Basin Report 1780 (Feb 1966).

considerations; however, such a section would have extremely small tolerance to variation in angle of attack before the inception of leading-edge cavitation; see Figure 10.

3. To provide a zero factor of safety from inception of back bubble cavitation at the ideal angle of attack and the cavitation number corresponding to the circumferential mean resultant inflow velocity and the blade vertical upward. However, such sections near the blade tip would experience back bubble and leading-edge sheet cavitation at angle of attack slightly different from the ideal angle of attack.

4. To provide the maximum cavitation-free bucket width at the cavitation number corresponding to the circumferential mean longitudinal velocity and the blade in the vertical upward position. This section, which is the "optimum" section described in Reference 23, will provide the maximum total angle of attack variation, considering both positive and negative angles, before inception of leading-edge sheet cavitation at this cavitation number. This approach results in a thinner blade section than the approach providing no factor of safety from back bubble cavitation, criterion (3), and, of course, provides greater safety from back bubble cavitation. However, leading-edge sheet cavitation will occur in the region from the 50-percent radius to the tip, even with this optimum section; see Figure 10.

For merchant ships, the primary adverse effects of cavitation are erosion and thrust breakdown. Both of these phenomena are more sensitive to back bubble cavitation than to leading-edge sheet cavitation. Cavitation erosion is considered to be caused primarily by the collapse of the cavitation bubbles on the surface of the blade and generally occurs in the presence of transient cloud or bubble cavitation.[24,25] Therefore, it is advantageous to eliminate back bubble cavitation and to accept some leading-edge sheet cavitation.

The final selection of the radial distribution of blade-section thickness and chordlength will necessarily be a compromise between cavitation, strength, and efficiency. Considering efficiency, it was desirable to limit the expanded-area ratio to no greater than 0.77. Therefore, calculations were undertaken to develop a satisfactory distribution of chordlength and thickness from blade root to tip.

For this purpose, cavitation and strength calculations were conducted on each of three analytically defined[21] distributions of chordlength for expanded-area ratio EAR = 0.77. The three blade outlines investigated represent different compromises between strength and cavitation. These blade outlines all have maximum chordlength at the 60-percent radius and have ratios of chordlength at the 20-percent radius to maximum chordlengths of 0.6, 0.7, and 0.8. Longer chordlengths near the root result in reduced stresses near the root where the peak stresses generally occur. However, for EAR held constant, longer chordlengths near the root

---

[24]Van Oossanen, P., "Cavitation Testing of Marine Propellers," Schip en Werf, Vol. 39, Nos. 13 and 14 (1972); also Netherlands Ship Model Basin Publication 418 (1972).

[25]Morgan, W.B. and J.Z. Lichtman, "Cavitation Effects on Marine Devices," American Society of Mechanical Engineers Cavitation State of Knowledge, pp. 195–241 (1969).

result in shorter chordlengths near the tip, tending to bring on back bubble cavitation at lower speeds near the tip.

The radial distribution of t/c was determined for each of these radial distributions of chordlength for EAR = 0.77 and the Type I radial distribution of loading (Figure 5) for each of two of the previously described cavitation criteria: zero factor of safety from back bubble cavitation at ideal angle of attack, criterion (3), and the optimum section which provides maximum cavitation-free variation in angle of attack at the specified cavitation number, criterion (4). As discussed previously, leading-edge sheet cavitation is predicted from the 50-percent radius to the blade tip for either of these two cavitation criteria. Therefore, to ensure freedom from back bubble cavitation, it was desirable to select the t/c in this region to be slightly less than that of the optimum foil. The radial distribution of t/c based on each of these criteria is presented in Figure 11 for the distribution of chordlength with the ratio of chordlength at the root to maximum chordlength of 0.6, the one finally selected. Similar curves were derived for the other two blade outlines; however, these have not been presented.

The stresses in the blade arising from both hydrodynamic loading and centrifugal loading at the full-power ahead condition were calculated by modified beam theory. The axis of the beam was assumed to be a radial line through the centroid of the blade section for which the stress was being calculated. At each radial position the cross section of the beam was assumed to be the constant-radius section, except that the camber was assumed to be zero. The camber was taken to be zero because substantial experimental data indicated that subcavitating propellers behaved structurally as if the blade sections were uncambered.[26] At each constant-radius section, the hydrodynamic loading was represented as a force vector normal to the axis of the beam and a moment vector parallel to the axis of the beam, torsion; the centrifugal loading was represented as a force vector parallel to the axis of the beam and a bending-moment vector normal to the axis of the beam. The principal stress was then calculated at selected points on the blade.

Using this method, the maximum value of the temporal mean stress—based upon the circumferential mean velocity at each radius—was calculated at each 0.1 radius for three blade outlines and two linear distributions of thickness. Figure 11 shows for one blade outline the maximum value of the temporal mean stress for two linear distributions of thickness with t/c at the 20-percent radius = 0.20 and 0.25 and a minimum thickness at the tip of 1.6 inches.

---

[26]McCarthy, J.H. and J.S. Brock, "Static Stresses on Wide Bladed Propellers," Journal of Ship Research, Vol. 17, No. 2, pp. 121–134 (Jun 1970).

From Figure 11 it is apparent that a linear distribution of thickness would have resulted in excessive thickness near the tip from considerations of back bubble cavitation. However, by superimposing an S-shaped curve on the linear distribution of thickness with t/c = 0.20 at the 20-percent radius, it was possible to meet the cavitation criterion dominant at the outer radii and the strength criterion dominant at the inner radii. Thus, the distribution of thickness was selected.

The stress at the inner radii could have been reduced by using either a longer chordlength, a thicker section, or both at the inner radii. The chordlength at the section at the hub was limited by the length of the hub and tailshaft arrangement on the ship. Section thickness at the inner radii was limited by blockage, due to the near proximity of adjacent blades, which could reduce both propeller efficiency and speed of cavitation inception in this region. Also, a t/c greater than approximately 0.20 tends to produce significant section form drag,[1] resulting in a decrease in propeller efficiency.

To calculate the fatigue life, unsteady propeller loading was calculated, using a computer program based on unsteady lifting-surface theory.[15] Unsteady loading and bending moments were calculated for each of the first nine harmonics of the wake. The unsteady stresses were then calculated, using the same procedure as was used for calculating steady stress.

Figure 12 shows the design stress point on a modified Goodman diagram.* This diagram indicates that the highly skewed propeller with the selected blade outline and thickness distribution possessed sufficient static strength and fatigue life for the specified material, i.e., nickel-aluminum bronze, ABS Type 4.[27]

In these strength calculations it was assumed that the maximum stress in the blade of the propeller would occur at full-ahead power, usually the condition of maximum propeller thrust. However, for some ships, the maximum stress may occur under transient conditions, such as either crash- or steady-astern operations. This will depend on the type of powerplant and the astern power available because with some powerplants the shaft torque may be momentarily greater than the maximum ahead torque. Where the maximum astern power is nearly equal to the maximum ahead power, the maximum stress might occur while going astern, especially for highly skewed propellers. Since the ship operates at only a very short time under transient or astern conditions, it is not necessary to consider fatigue strength for these conditions; it is only necessary to ensure that yield stress is not exceeded. At full-ahead power, the propeller under consideration in this report has a substantial factor of safety for yield stress; see Figure 12. Therefore, it is considered quite unlikely that the propeller will

---

*The material properties for nickel-aluminum bronze as shown in Figure 12 are based on unpublished data from the International Nickel Company, Inc.

[27] American Bureau of Shipping, "Rules for Building and Classing Steel Vessels," p. 621 (1972).

15

fail under transient or astern operation. In an attempt to substantiate this, the stress was experimentally determined on a model of the highly skewed propeller at simulated ahead and astern operation. The experiments are discussed in the section on design verification.

FINAL GEOMETRY

Next, the final camber and pitch distributions were determined, using the lifting-surface procedure of Cheng[28] together with the thickness corrections of Kerwin and Leopold.[29] It is emphasized that the pitch correction due to skew is substantial, and a skewed propeller with the desired radial distribution of loading can be properly designed only by the use of lifting-surface techniques. Reference 2 presents pitch- and camber-correction factors, derived from lifting-surface theory,[28,29] for highly skewed propellers.

The final propeller geometry provided a minimum clearance of slightly more than 2 feet, 8 percent of the diameter, between the propeller and rudder for a longitudinal propeller location the same as that of the currently installed propeller. The clearance for the presently installed propeller is approximately 3.5 feet. Clearance between the propeller and rudder can have a substantial influence on propeller-induced vibration; however, for a given ship it is not clear how much clearance should be used.[11,30,31] Reference 31 clearly shows that the unsteady loading on the rudder does not monotonically decrease with increasing clearance between the propeller and the rudder. Unpublished results at the Center indicate that skew may reduce the unsteady loading induced on the rudder by the propeller at a given clearance. If desired, the clearance between the highly skewed propeller and the rudder could have been increased by raking the blades forward. This was not done in the design presented here. Lifting-surface propeller design techniques capable of considering the influence of substantial forward rake have recently become available.[32,33]

Finally, a strength check was made with the final geometry, including lifting-surface corrections. This check confirmed the stress level calculated before the lifting-surface corrections; see Figure 12. This completed the design process.

---

[28]Cheng, H.M., "Hydrodynamic Aspect of Propeller Design Based on Lifting-Surface Theory," Parts 1 and 2, David Taylor Model Basin Reports 1802 and 1803 (Sep 1964 and Jun 1965).

[29]Kerwin, J.E. and R. Leopold, "A Design Theory for Subcavitating Propellers," Transactions of Society of Naval Architects and Marine Engineers, Vol. 72, pp. 294–335 (1964).

[30]Breslin, J.P., "Theoretical and Experimental Techniques for Practical Estimation of Propeller-Induced Vibratory Forces," Transactions of Society of Naval Architects and Marine Engineers, Vol. 78, pp. 23–40 (1970).

[31]Lewis, F.M., "Propeller Excited Hull and Rudder Force Measurements," Massachusetts Institute of Technology, Department of Ocean Engineering Report 73-10 (Apr 1973).

[32]Kerwin, J.E., "Computer Techniques for Propeller Blade Section Design," Proceedings of the Second Lips Propeller Symposium, Drunen, Holland, pp. 7–31 (May 1973).

[33]Pien, P.C., Discussion of Paper "Highly-Skewed Propellers," by Cumming, Morgan and Boswell, Transactions of Society of Naval Architects and Marine Engineers, Vol. 80 (1972).

Table 2 presents the principal geometric characteristics of the propeller; Figure 13 is a drawing of the propeller; Figure 14 shows a model propeller built to this design; and Figure 15 shows this model propeller fitted to a model of the hull.

DESIGN VERIFICATION

Model experiments were conducted to evaluate the highly skewed propeller design, considering self-propulsion performance, cavitation including erosion, and strength. Three model propellers were used in these experiments.

1. For cavitation and self-propulsion evaluation, a 10.32 inch-diameter aluminum model of the highly skewed design was used. This propeller of the same scale as the model hull was Center Model 4452.

2. For comparative cavitation and self-propulsion evaluation, a 10.32-inch-diameter aluminum model of the propeller currently fitted to the ship was used. This propeller, also the same scale as the model hull, was Center Model 4295; Figure 16.

3. For strength evaluation, a 20-inch-diameter propeller was used made of nickel-aluminum bronz, ABS Type 4,[27] the same material as the prototype. This propeller constructed with two blades rather than six for economic reasons, was Center Model 4453.

PROPULSION EVALUATION

Self-propulsion experiments were conducted at design trim and displacement with propeller Models 4452 and 4295 fitted to the model hull, representing this ship, Center hull Model 5091-1; see Figure 15. The corresponding resistance experiments of Model 5091-1 and open water experiments of propeller Models 4452 and 4295 were conducted to allow derivation of the appropriate propulsion coefficients.

Table 3 compares the self-propulsion experimental results for the two propellers at design delivered horsepower P_D = 30,000. This comparison shows that the self-propulsion performance of the two propellers is equivalent, except for rpm which has been designed to be different.

The results indicate that at full power, the highly skewed propeller will turn at 109 rpm. This tends to confirm the design technique from considerations of propulsion.

CAVITATION AND EROSION EVALUATION

The highly skewed propeller was evaluated for cavitation performance, including cavitation erosion, by experiments using propeller Model 4452 in the 24-inch variable pressure water tunnel at the Center. For comparison, cavitation performance but not cavitation erosion was evaluated by the same techniques, using a model of the propeller currently installed on the ship, Model 4295; erosion experiments had been conducted previously on Model 4295.

17

TABLE 2 – GEOMETRIC CHARACTERISTICS OF HIGHLY SKEWED PROPELLER

Diameter	23 feet
Section Meanline	NACA a = 0.8 (see Reference 23)
Section-Thickness Distribution	NACA 66 with NSRDC modified nose and tail (see Reference 23)
Expanded Area Ratio	0.770
Projected Area Ratio	0.615
Mean Width Ratio	0.244
Blade-Thickness Fraction	0.056
Rake	0
Projected Skew Angle at Blade Tip	60 degrees

r/R	c/D	P/D	θ_s	t/D	f_M/D
0.2	0.2013	1.1450	0.000	0.0400	0.0140
0.3	0.2379	1.1462	7.500	0.0378	0.0119
0.4	0.2648	1.1493	15.000	0.0339	0.0084
0.5	0.2816	1.1574	22.500	0.0287	0.0069
0.6	0.2876	1.1448	30.000	0.0229	0.0065
0.7	0.2807	1.0937	37.500	0.0171	0.0057
0.8	0.2564	1.0188	45.000	0.0120	0.0042
0.9	0.2029	0.9416	52.500	0.0080	0.0025
0.95	0.1528	0.9040	56.250	0.0066	0.0014
1.00	0.0000	0.8659	60.000	0.0055	0.0000

TABLE 3 – POWERING CHARACTERISTICS AT DESIGN POWER OF HIGHLY SKEWED PROPELLER AND PROPELLER CURRENTLY ON SHIP

	Highly Skewed Propeller Model Propeller 4452	Propeller Currently Fitted Model Propeller 4295
Ship Speed V	24.60	24.59
Rotational Speed RPM	109.00	112.90
Propeller Efficiency Behind Hull η_B	0.68	0.68
Propulsive Efficiency η_D	0.74	0.74
Taylor Wake $1-w_T$	0.78	0.78
Thrust Deduction $1-t$	0.84	0.84
Advance Coefficient J	0.78	0.75
Thrust-Loading Coefficient C_{Th}	0.80	0.80

18

For these experiments the propellers were anodized, dyed black, and marked with a grid pattern for visual aid. These experiments were conducted in a simulated wake pattern produced by wire grid screens.[34] These screens were especially designed and constructed to produce the longitudinal wake distribution existing behind the hull in the plane of the propeller. Figure 17 shows the wake screen and propeller Model 4452 at its proper transverse position.

For both propellers experiments were conducted over the simulated self-propulsion range to determine cavitation inception at various radii, cavitation patterns at simulated ship speeds, and thrust breakdown due to cavitation. For the highly skewed propeller, Model 4452, the erosion experiments were conducted by running Model 4452 for 43 hours at the simulated full-power ahead condition.

Figure 18 presents graphs showing cavitation inception at various radii for Models 4452 and 4295 operating in the simulated wake field. The graphs for the inception of tip-vortex cavitation have been corrected for the difference in Reynolds number between model and full scale using the data presented in Reference 35. The graphs reflect the maximum cavitation observed for each revolution. For both propellers, the leading-edge sheet cavitation started at the blade tip and progressed toward the blade root with increasing simulated ship speed. A graph marked with a given blade radius indicates that cavitation is predicted from the marked radius to the tip.

These data indicate that the highly skewed propeller will delay the inception of back- and face-sheet cavitation by approximately 2 knots and visual tip-vortex cavitation by approximately 3 knots, relative to the propeller currently installed on the ship. The predicted delay in the inception of back and face leading-edge cavitation by 2 or more knots by applying high skew is consistent with previous results obtained at the Center on a series of skewed propellers in uniform flow.[6,7] The predicted delay in the inception of visual tip-vortex cavitation is due to unloading the blade tip of the highly skewed propeller, relative to the propeller currently installed on the ship; see Figures 13 and 16. No back bubble cavitation was observed on either propeller for any of the conditions evaluated.

These inception data qualitatively confirm the use of two-dimensional characteristics during the design process for evaluating the inception of leading-edge sheet cavitation and back bubble cavitation. These results tend to confirm that the compromise in design to suppress back bubble cavitation and to accept leading-edge sheet cavitation from the 50-percent radius to the tip will be realized.

---

[34]McCarthy, J.H., "Steady Flow Past Nonuniform Wire Grids," Journal of Fluid Mechanics, Vol. 19, Part 4 (1964).

[35]McCormick, B.W., Jr., "On Cavitation Produced by a Vortex Trailing from a Lifting Surface," Journal of Basic Engineering, Vol. 84, Series D, No. 3, pp. 369–379 (Sep 1962).

Figures 19 through 21 present sketches of the cavitation observed on a highly skewed propeller when simulating 22, 24.5, and 26 knots. The sketches show the various patterns of cavitation encountered by the blades in each revolution through the nonuniform flow. The back cavitation was generally the most extensive at the blade angular position, at which the tip was approximately 15 degrees past the vertically upward position. This is consistent with previous data.[36] Face cavitation was generally the most developed where the angles to the leading edge of the local radius were 90 and 270 degrees. These are the positions in the propeller disk at which the maximum values of longitudinal velocity and negative angles of attack occur; see Figure 2. The cavitation patterns on the model of the propeller currently installed on the ship were similar to those on the highly skewed model propeller, except that the chordwise extent of the cavity was greater.

Figure 22 shows the tip of one of the blades of propeller Model 4452 after 43 hours of simulated full-power operation. This is typical of the simulated erosion on all of the blades; see Figure 14. This slight simulated erosion occurred on the back of the blades in the region from the 90-percent radius to the tip and over the 25-percent chord nearest the trailing edge. The patterns appearing on Figure 22 are caused by erosion of the black dye applied during the anodizing process. The surface remained smooth, and there was insignificant pitting in the metal.

Erosion experiments of this type are qualitative in nature. There is no definite information available concerning scaling the depth of erosion or the time that it takes for erosion to occur. Therefore, it can be cautiously stated that this design may have a minor erosion problem. Based upon results from comparative model erosion experiments of the propeller currently installed on the ship, which have not been presented, it would be expected that the erosion would be less on the highly skewed propeller than on the propeller presently installed.

During the design process, an attempt was made to minimize erosion by avoiding back bubble cavitation and minimizing the extent of leading-edge, back-sheet cavitation. Visual observations of cavitation indicated that these objectives were achieved on the model; however, erosion would still be predicted.

At the design condition the leading-edge sheet cavitation collapsed where the erosion patterns occurred for some blade angular positions in the wake; see Figure 20. The breaking-up and collapsing of the sheet cavitation is known to cause erosion in many cases.[24,25] This phenomenon often occurs with "cloud" cavitation. However, no cloud cavitation was observed in the experiments described here. The severity of the variation of the wake with

[36]Ito, T., "An Experimental Investigation into the Unsteady Cavitation of Marine Propellers," Ship Research Institute Paper 11, Tokyo, Japan (Mar 1966).

blade angular position prohibits avoiding erosion by forcing sheet cavitation to collapse downstream of the trailing edge of the blade. This could be accomplished at some, but not all, blade angular positions.

The model results have indicated that thrust breakdown due to cavitation will not occur at full-power for either the highly skewed propeller or the propeller currently installed on the ship.

STRENGTH EVALUATION

To evaluate the strength of the highly skewed propeller, strain measurements were made on a model propeller operating under simulated ahead and astern conditions. For these experiments a two-bladed, 20-inch-diameter model of the highly skewed design was constructed of nickel-aluminum bronz, ABS Type 4,[27] the material specified for the full-scale propeller. This propeller was Model 4453. Making the model of the same material as the prototype allowed simultaneous scaling of hydrodynamic loading, centrifugal loading, strain, stress, and stress as a fraction of yield stress. The appropriate scaling parameter was the Cauchy number $\rho V^2/E$. For a scaled hydrodynamic flow field having the same wake pattern and mean advance coefficient, the magnitude and distribution of all the previously described parameters would be the same on model and full-scale propeller, provided the effective speed of advance were the same on model and full scale, and provided the model and full scale were made of the same material. A two-bladed propeller was used to reduce the cost of model construction. A 20-inch-diameter model propeller was used instead of a smaller model to allow sufficient spatial resolution of the strain measurements as well as to minimize disturbance to the flow caused by the strain gages and the associated waterproofing material.

Experiments were conducted in uniform flow in the 36-inch, variable pressure water tunnel at the Center for normal ahead operation at designed mean advance coefficient $J = 0.78$ and steady backing operation at $J = 0.5$ and 0.7. For each advance coefficient, the propeller was evaluated over a range of thrust to somewhat more than simulated full-scale thrust at design ahead power, scaled by the Cauchy number $\rho V^2/E$, with cavitation number held constant. For each advance coefficient the cavitation number was selected as the maximum obtainable in the facility at the highest loading condition to be evaluated. At design advance coefficient, experiments were also conducted at design cavitation number.

The strain was measured with strain gages and strain rosettes placed along the 30-percent radius just outside the root fillet. The measurements were restricted to the 30-percent radius because (1) this was the region in which the largest stresses were expected to occur under normal ahead and steady astern operation, and (2) the disturbance to the flow from the gages and waterproofing was minimum in this region of the blade. Limitations of readily available instrumentation restricted the total number of gages to 16. Therefore, it was

21

necessary to select the location and orientation of the gages judiciously so that maximum information would be obtained. Figure 23 shows the locations selected for the gages. The single gages were oriented to measure strain in the radial direction. However, for a complex structure such as a highly skewed propeller, in which the direction of the principal stresses is not known beforehand, it is not possible to accurately calculate stress from strain measured in only one direction. Strain data from the single strain gages were used only to check that the measured strain distribution was reasonable and that the stresses determined by the rosettes were a good representation of the maximum stress in the blade for each mode of operation.

The experimental maximum principal stresses for Cauchy scaled conditions corresponding to full power ahead and astern, assuming astern rpm is 50 percent of full-ahead rpm, are shown in Figure 24. Data from the single strain gages on the face and back of the blade suggest that the maximum principal stresses on the face and back of the blade are approximately equal in absolute value but opposite in sense. This is consistent with other data.[37,38] Assuming that the maximum principal stresses on the face and back are equal and opposite, the results indicate that the maximum principal tensile stress in astern operation will be only about 30 percent of the maximum principal tensile stress in ahead operation. For both ahead and astern operation, the maximum principal stress occurred near the trailing edge. This is consistent with other available data on highly skewed propellers which are for propellers loaded statically with uniform air pressure.[37,38] The similarity of stress patterns implies that neither the centrifugal loading nor the spatial variation in the hydrodynamic loading drastically affects the stress distribution near the blade root.

For the full-ahead advance coefficient, the results showed no measureable influence of cavitation on stresses up to cavitation-scaled, full-power speed. This was reasonable, since there was no thrust breakdown due to cavitation up to full-power speed.

At the design condition it was desirable to compare the measured stresses with the design calculated stresses. However, at designed advance coefficient the load distribution on the model propeller differed from the design load distribution because (1) the experiment was conducted in uniform flow, whereas the propeller was designed to operate in a radially varying flow field, and (2) the model propeller had only two blades, whereas the design was for six blades. However, correlation between measured and calculated stress was obtained as follows: the load distribution was calculated for the two-bladed propeller in uniform flow at design advance coefficient by using a recently developed performance-prediction computer

---

[37]Boswell, R.J., "Static Stress Measurements on a Highly-Skewed Propeller Blade," NSRDC Report 3247 (Dec 1969).

[38]Boswell, R.J. et al., "Experimental Measurements of Static S   es in a Series of Research Skewed Propellers with and without Forward Rake," NSRDC Report 3804 (in preparation).

22

program based upon lifting-surface techniques.[39] The calcu. d net performance—thrust, torque, and efficiency—of the two-bladed propeller was in good agreement with experimental results. Stress calculations were then performed for the two-bladed propeller, using the calculated load distribution and the same stress-calculation techniques as in the design process. Correlation between theory and experiment were thus made for the same condition, which differed from the true design condition only in that the radial load distribution was slightly different.

There is no reason to expect that the trends of the experimental data for the two-bladed propeller are significantly different from what the trends might be for a six-bladed propeller. Thus, the measured locations of maximum stress and relative magnitudes of stresses at various operating conditions measured on the two-bladed model should be directly applicable to the six-bladed design.

The results generally confirmed the stress calculation procedure and indicated that the highly skewed propeller would possess adequate strength for full-power ahead and steady astern operation. At design ahead advance coefficient, the highest experimental principal stress at the 30-percent radius was 6100 psi—extrapolated value at trailing edge was 7100 psi— whereas the calculated maximum principal stress at the 30-percent radius was 8500 psi. This implies that the stress-calculation technique, using modified beam theory, yields results which are roughly 20-percent too high, i.e., the calculation is conservative. Hence, the factor of safety in the highly skewed propeller is greater than that indicated in Figure 12.

Experimental deflection patterns on highly skewed propellers loaded with static air pressure show that highly skewed propellers tend to deflect so that the pitch of the blades decreases slightly for ahead operation and increases slightly for astern operation.[40] The increase in pitch under astern operation tends to increase the hydrodynamic loading on the blade. This is the kind of deflection that can lead to static divergence.[41,42,43]* The air load experiments indicated that the static divergence speed decreased with increasing skew; however, the experiments yield no indication of the magnitude of the divergence speed.

In the structural experiments described in this section the hydrodynamic loading and elastic response of the blade were simultaneously scaled. These factors were the basic

---

[39]Cummings, D.E., "Numerical Prediction of Propeller Characteristics," Journal of Ship Research, pp. 12–18 (Mar 1973).

[40]Dhir, S.K. and J.P. Sikora, "Holographic Displacement Measurements on a Highly-Skewed Propeller Blade," NSRDC Report 3680 (Aug 1971).

[41]Abramson, H.N. et al., "Hydroelasticity with Special Reference to Hydrofoil Craft," NSRDC Report 2557, p. 443 (Sep 1967).

[42]Bisplinghoff, R.L. et al., "Aeroelasticity," Addison-Wesley Publishing Company, Inc., Reading, Massachusetts (1955) p. 483.

[43]Diedrich, F.W. and B. Budiansky, "Divergence of Swept Wings," National Advisory Committee for Aeronautics Technical Note 1680 (Aug 1948).

*Static divergence is static instability of lifting surface at a speed called the divergence speed, at which elasticity of lifting surface plays an essential roll in instability. Divergence is a closed-loop phenomenon in that the structural deformations resulting from the hydrodynamics forces give rise to additional hydrodynamic forces, which then modify the structural deformations, etc.

parameters controlling divergence speed. The propeller was loaded to several times its structurally scaled astern power, scaling parameter is $\rho V^2/E$, without divergence or significant blade deflection. Therefore, static divergence at steady astern operation appears to be no problem for the highly skewed propeller described in this report.

The experimental strength evaluation did not include consideration of the transient stresses encountered during the crash-astern maneuver. During this maneuver, which involves changing the propeller rotational speed from full ahead rpm to full astern rpm as quickly as practicable, high hydrodynamic loading may occur in the vicinity of the tip of the blade. This high loading, which results from very low pressure near the trailing edge on the face of the blade, may produce high local stresses in the vicinity of the blade tip, and, possibly, may cause the blade tips to bend over due to the local stresses exceeding the yield stress. Since these conditions endure only a very short time, fatigue does not enter into the problem. Static divergence may be a contributing factor, since the blade deflection tends to increase the hydrodynamic loading for astern rotational speed. However, for the cargo ship application considered in this report, cavitation will significantly reduce the high hydrodynamic loading near the tip—the pressure cannot be less than vapor pressure—and therefore, diminish the probability of failure during the crash astern maneuver.

CONCLUSIONS

From the design and model evaluation, the following conclusions have been drawn about the highly skewed propeller.

1. It will meet its design propulsion requirements.

2. It will possess propulsion performance comparable to that of the low-skew propeller currently installed on the ship.

3. Compared to the low-skew propeller currently installed on the ship, it will delay the inception of back, face, and tip vortex cavitation by 2 knots or more.

4. Compared to the low-skew propeller currently installed on the ship, it will possess less tendency towards cavitation erosion.

5. It will have adequate strength from considerations of mean and fatigue stresses at full-power ahead operation and mean stress and static divergence at steady-astern operation. However, the strength has not been evaluated under crash-astern operation.

6. Calculations indicate that the highly skewed propeller will produce lower vibration-excitation forces than the propeller currently fitted to the ship. Calculations, using unsteady lifting-surface theory, indicate that the highly skewed propeller will reduce blade-frequency thrust and torque by 90 percent, will reduce blade-frequency transverse horizontal bearing force by 60 percent, and will increase blade-frequency vertical bearing force by 2 percent, compared to the propeller currently installed on the ship.

24

RECOMMENDATIONS

It is recommended that the highly skewed propeller design be constructed full scale and that trials be conducted using this propeller to evaluate its performance, considering propulsion, cavitation, cavitation erosion, strength, and propeller-induced vibration. The blade strength should be evaluated at full-power ahead, full-power astern, and under the crash-astern maneuver. For comparison, similar trials should be conducted with the propeller currently fitted on the ship.

ACKNOWLEDGMENTS

Figure 1 — Hull Lines

Figure 2 -- Circumferential Distribution of Wake in Propeller Disk at r/R = 0.7

26
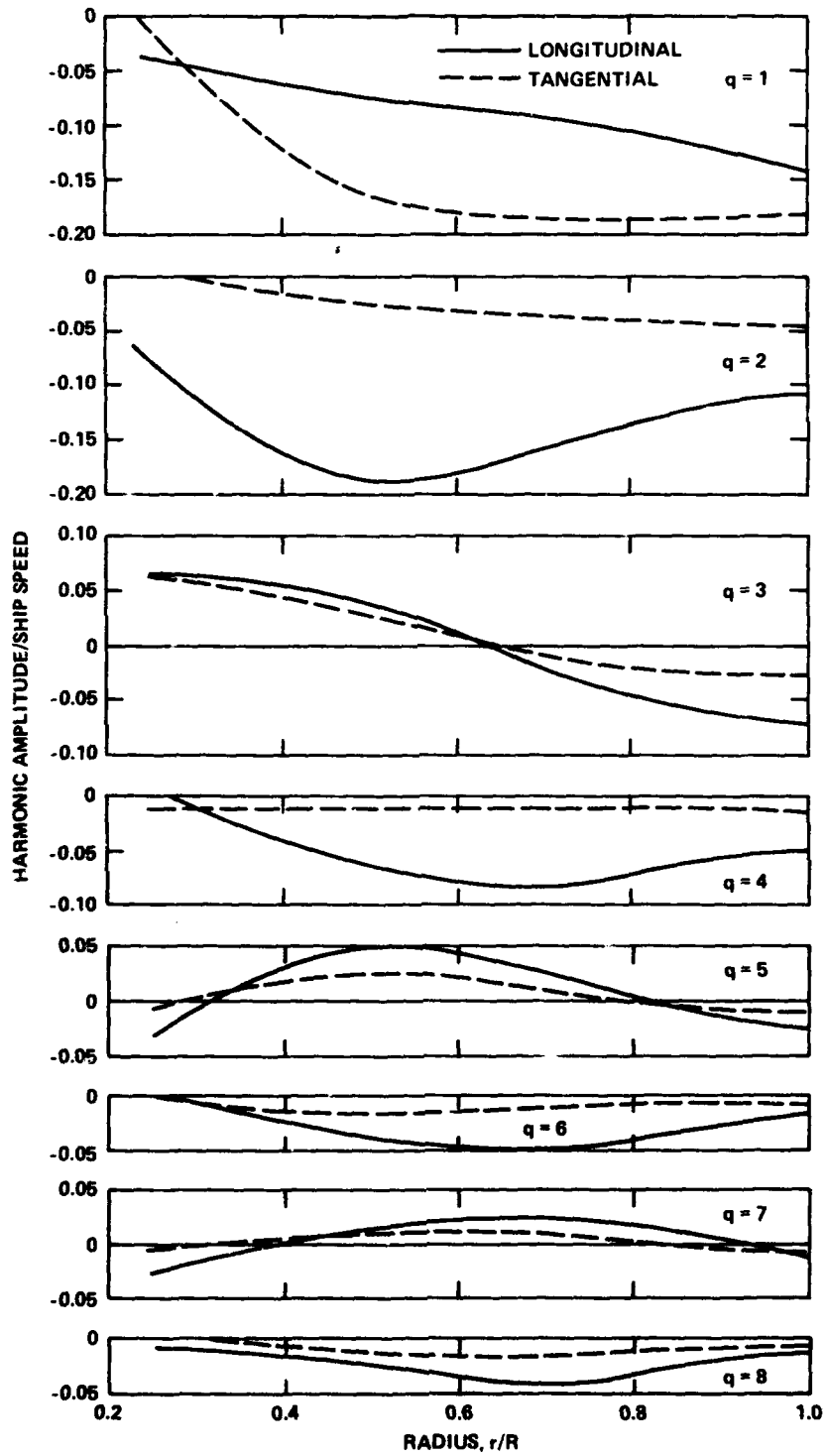
Figure 3 — Harmonic Amplitudes of Wake Velocities

27
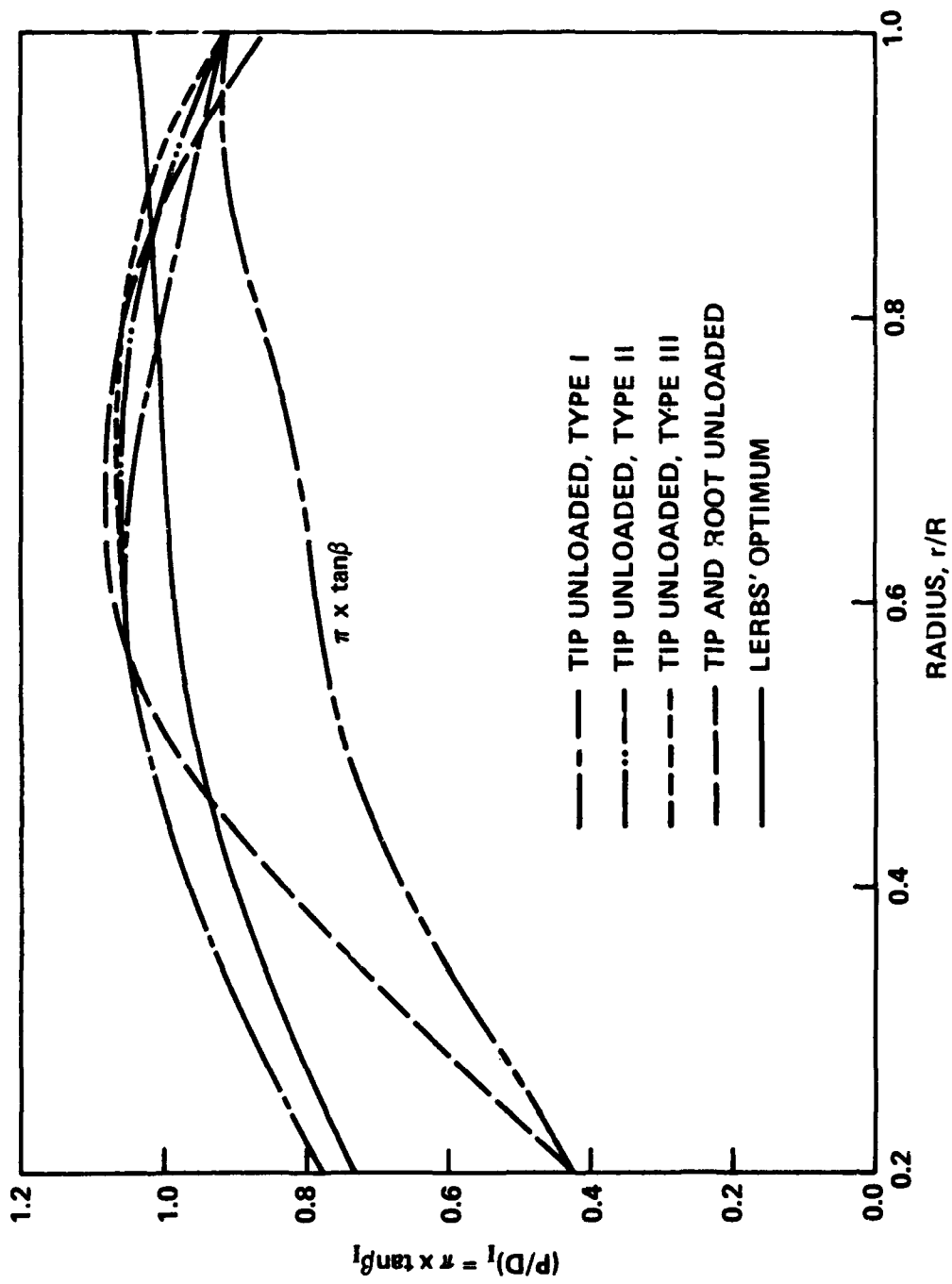
Figure 4 — Radial Distributions of Hydrodynamic Flow Angle
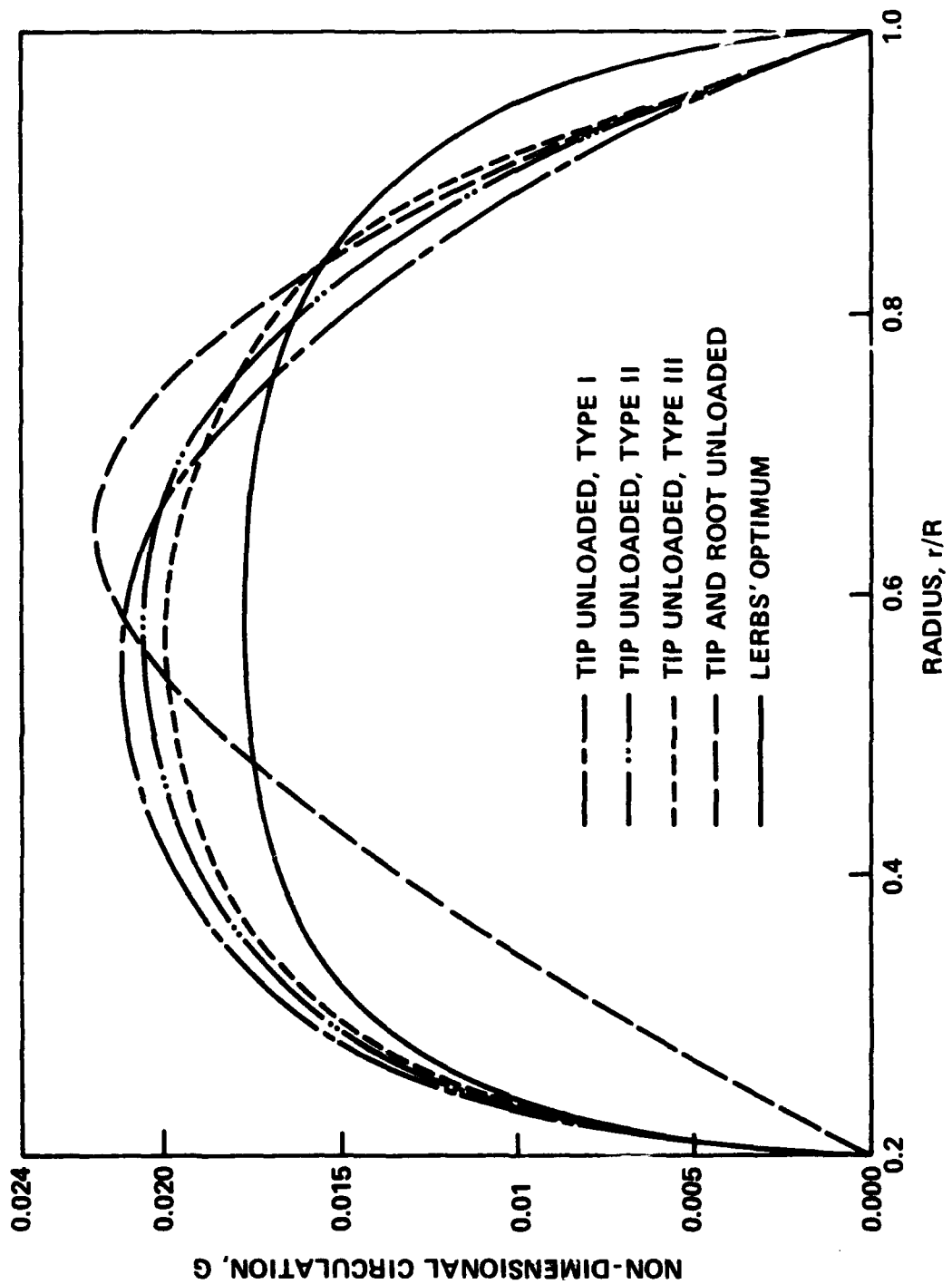
Figure 5 – Radial Distributions of Circulation

Legend:
- TIP UNLOADED, TYPE I
- TIP UNLOADED, TYPE II
- TIP UNLOADED, TYPE III
- TIP AND ROOT UNLOADED
- LERBS' OPTIMUM

X-axis: RADIUS, r/R (0.2 to 1.0)

Y-axis: NON-DIMENSIONAL CIRCULATION, G (0.000 to 0.024)
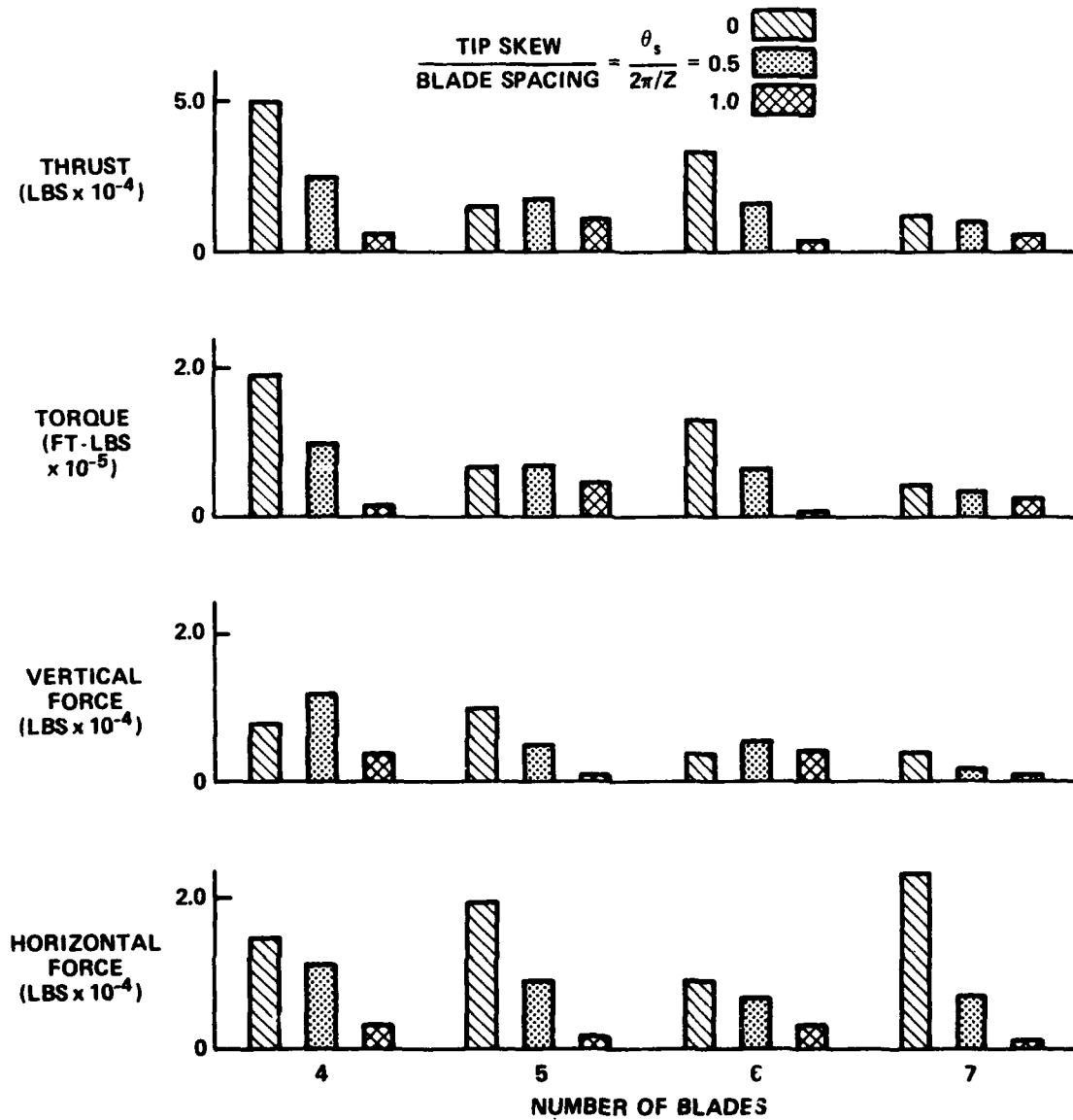
Figure 6 – Effect of Number of Blades and Linear Skew on Blade-Frequency Bearing Forces

30

SKEW DISTRIBUTION (1)   SKEW DISTRIBUTION (2)
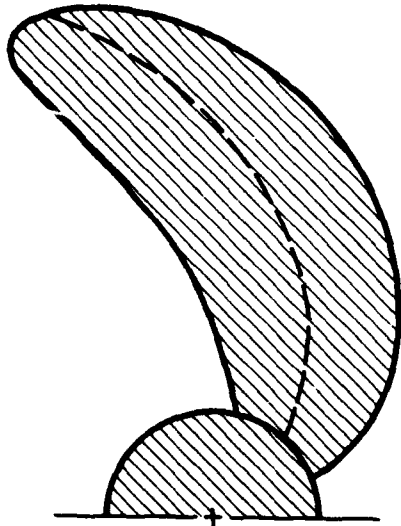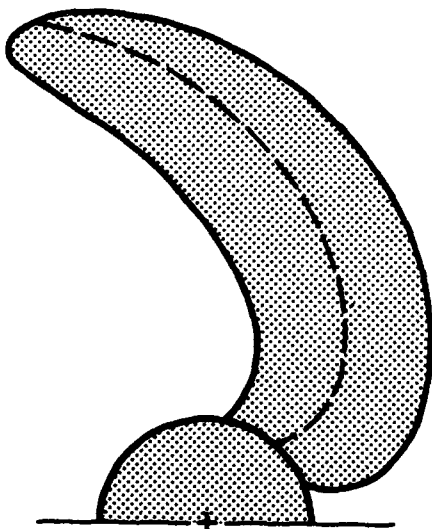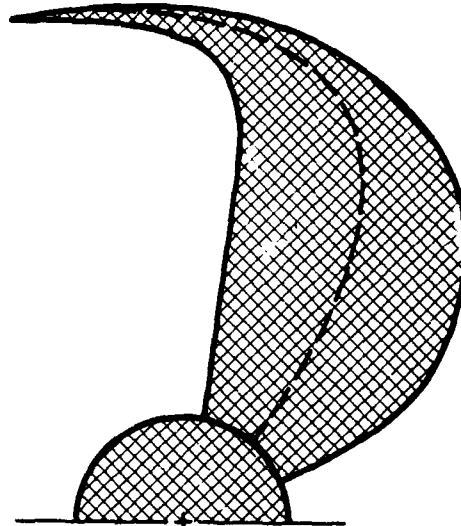
SKEW DISTRIBUTION (3)   SKEW DISTRIBUTION (4)
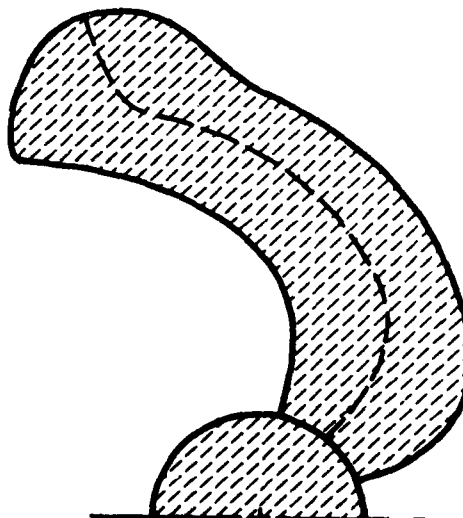
Figure 7 — Radial Distributions of Skew Investigated for Six-Bladed Propeller
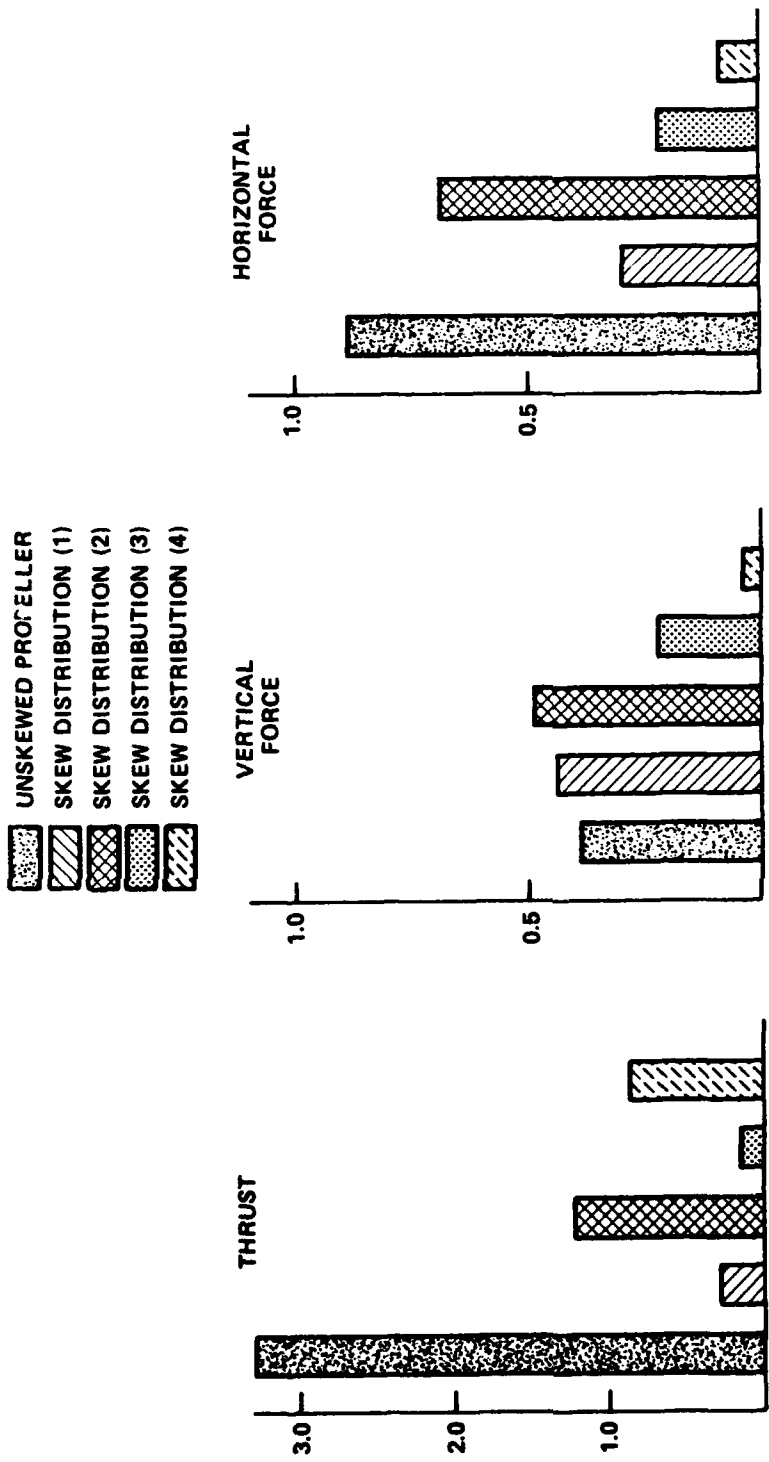
Figure 8 – Effect of Radial Distributions of Skew on Blade-Frequency Bearing Forces for Six-Bladed Propeller

32
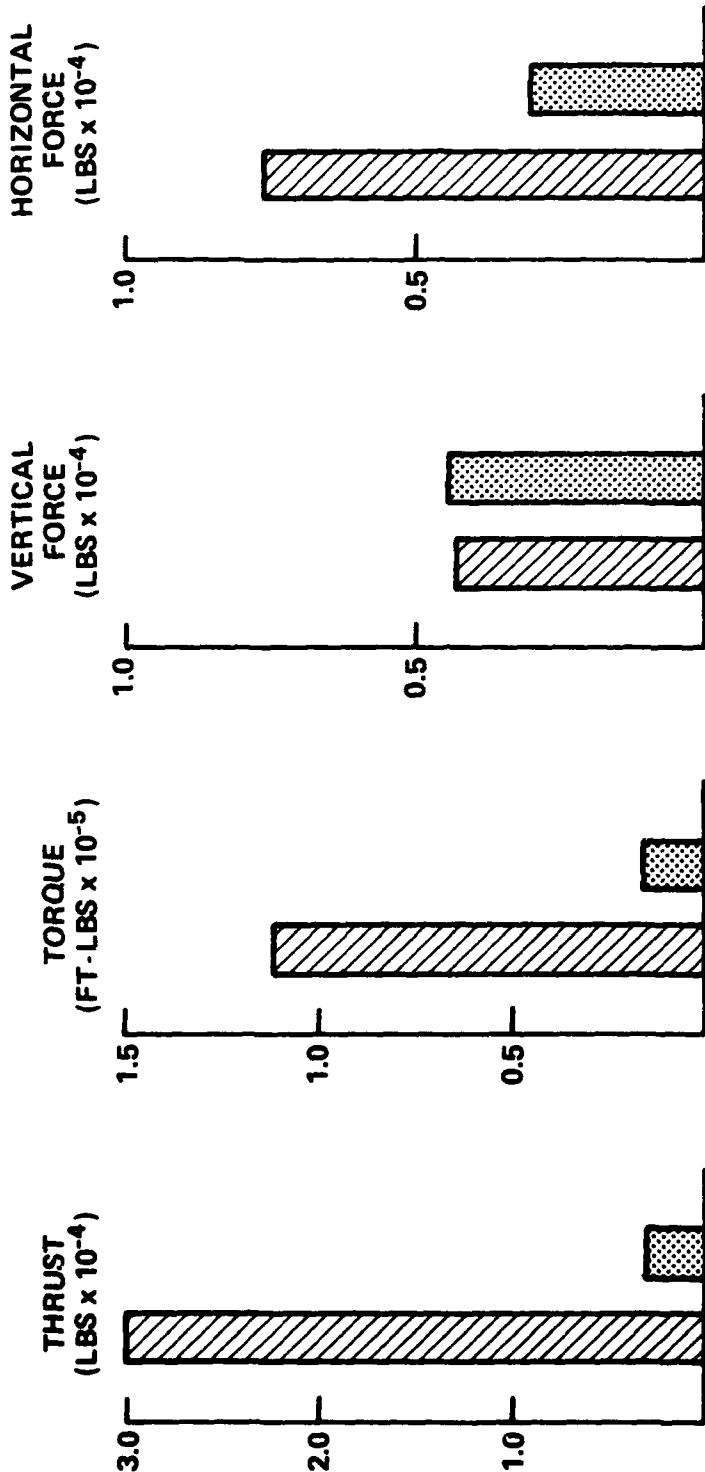
Figure 9 — Blade-Frequency Bearing Forces on Highly Skewed Propeller and Propeller Currently on the Ship

33

NACA 66 (TMB MOD NOSE AND TAIL)
NACA a = 0.8 CAMBERLINE
CAMBER RATIO = 0.02
t/c = 0.18

BACK SHEET

FACE SHEET

BACK BUBBLE

0.10
0.02
3.0
0.02
0.10
0.18

σ_r

2.0

1.0

0.3R
0.4R
0.5R
0.7R
0.9R

ANGLE OF ATTACK, DEG.

6
4
2
0
-2
-4
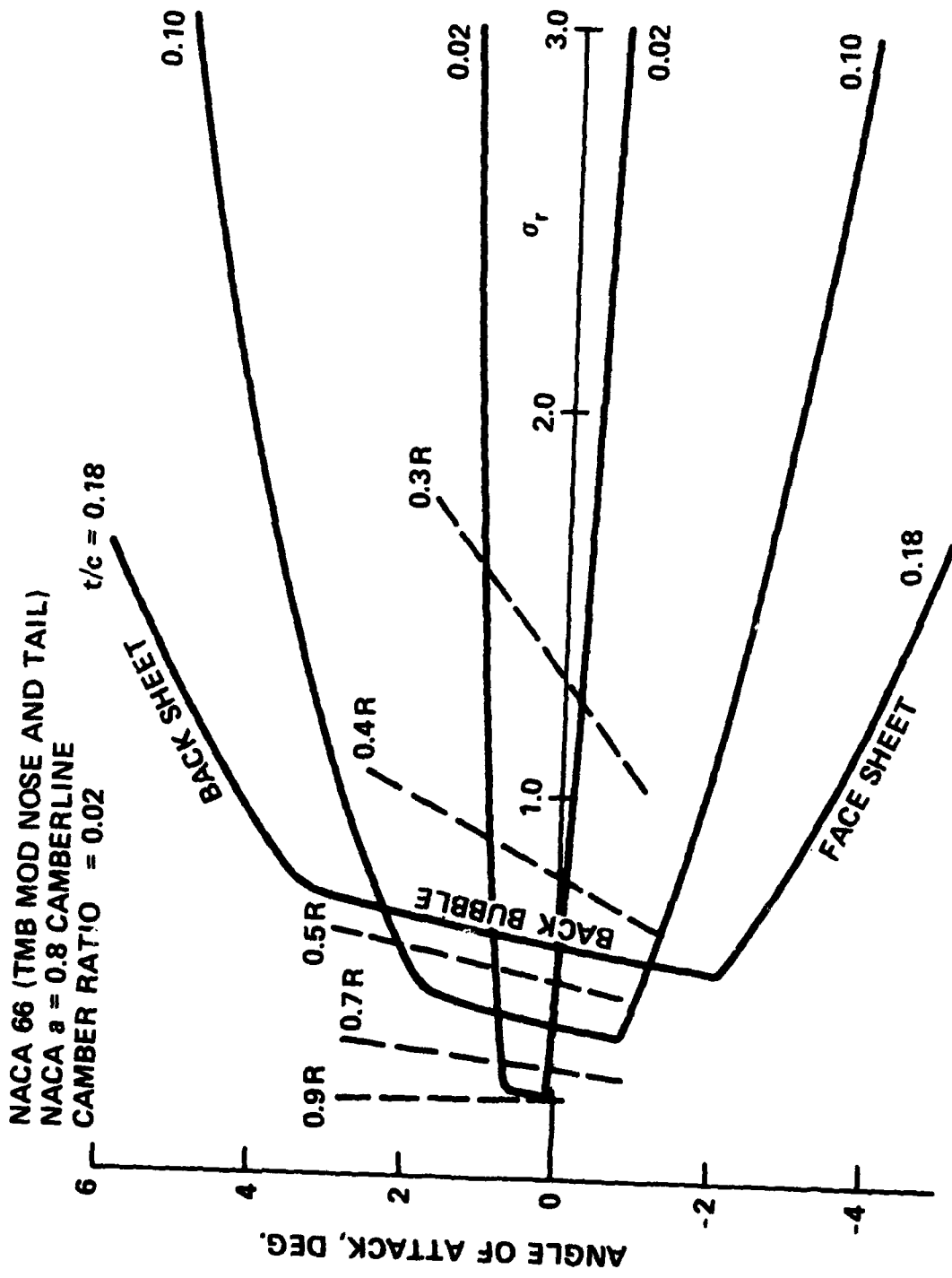
Figure 10 — Characteristic Cavitation Envelopes

34
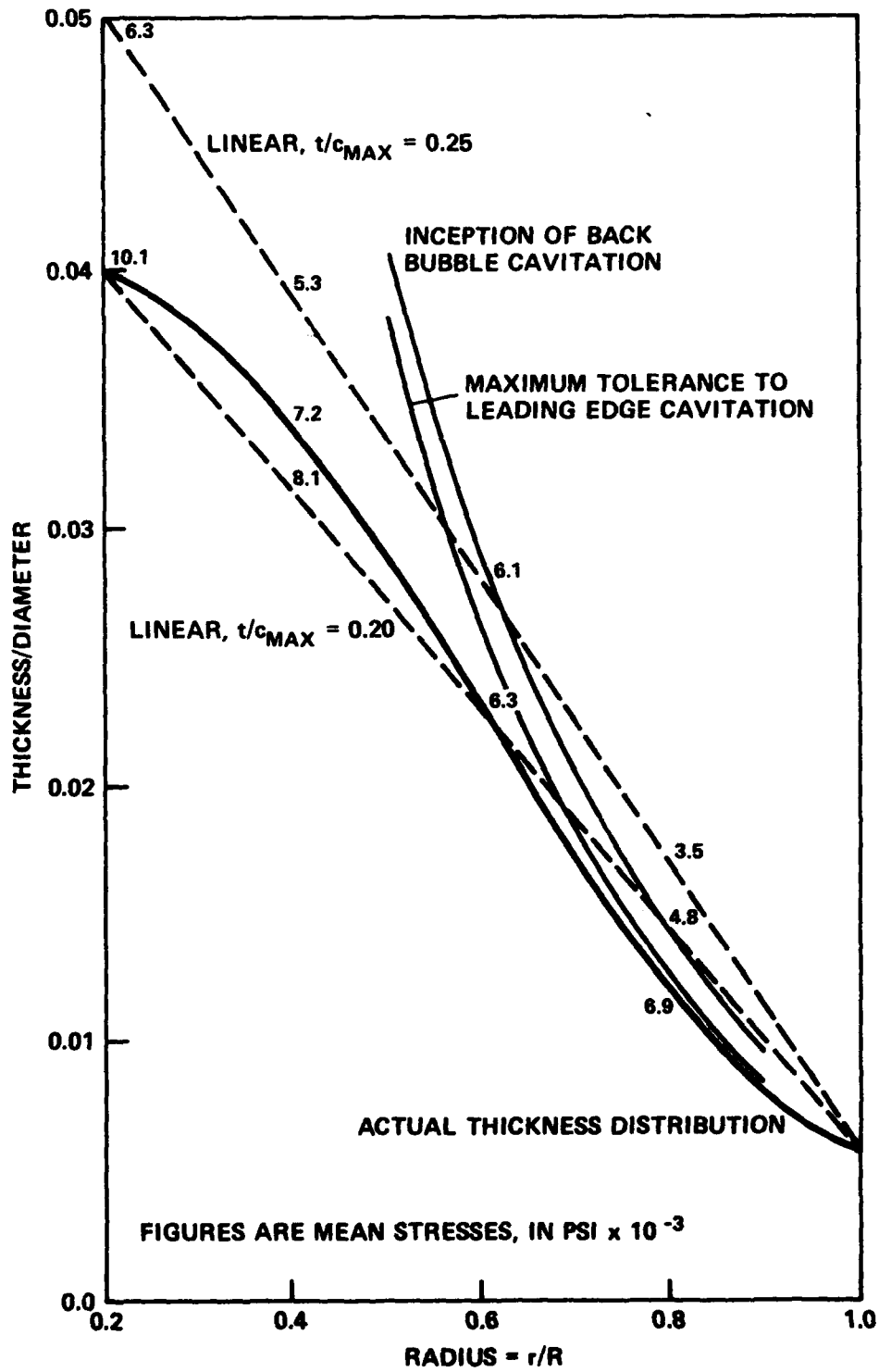
Figure 11 — Radial Distribution of Thickness, Based on Strength and Cavitation Criteria
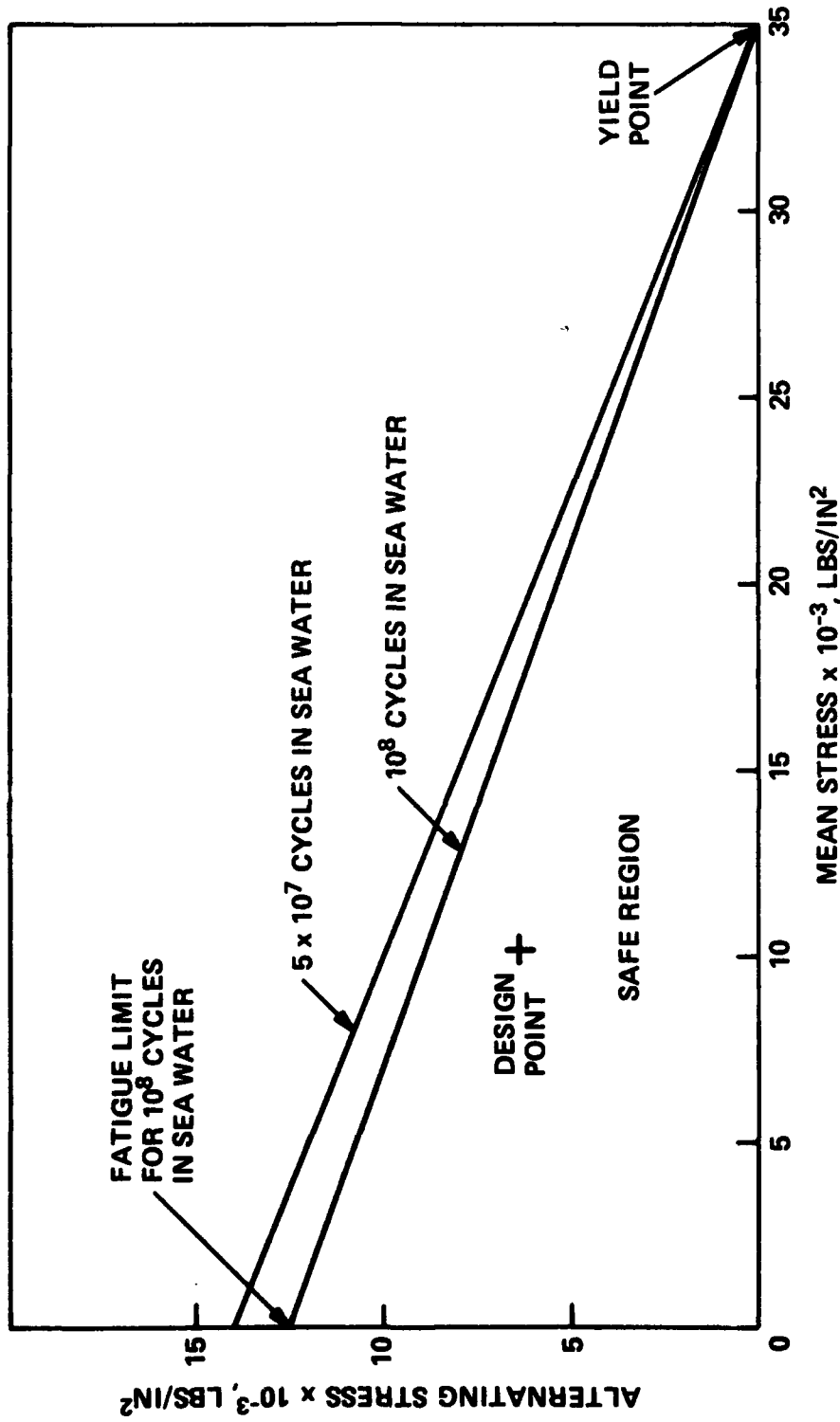
Figure 12 – Design Stress on a Modified Goodman Diagram

36

r/R	P/D
1.0	0.866
0.95	
0.9	0.942
0.8	1.019
0.7	1.094
0.6	1.145
0.5	1.157
0.4	1.149
0.3	1.140
0.2	1.145
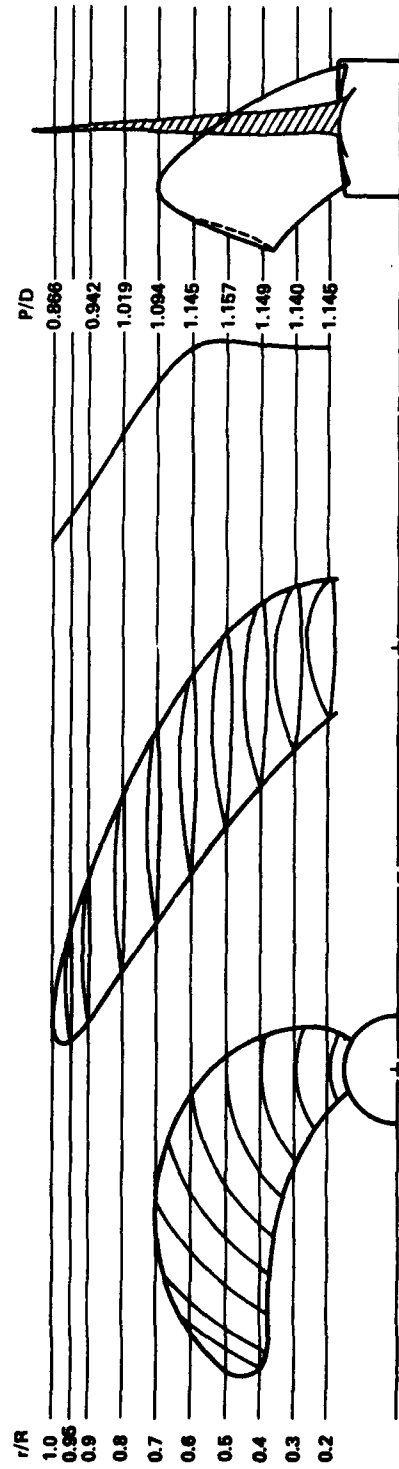
6 BLADES

Figure 13 — Highly Skewed Propeller, Schematic

37
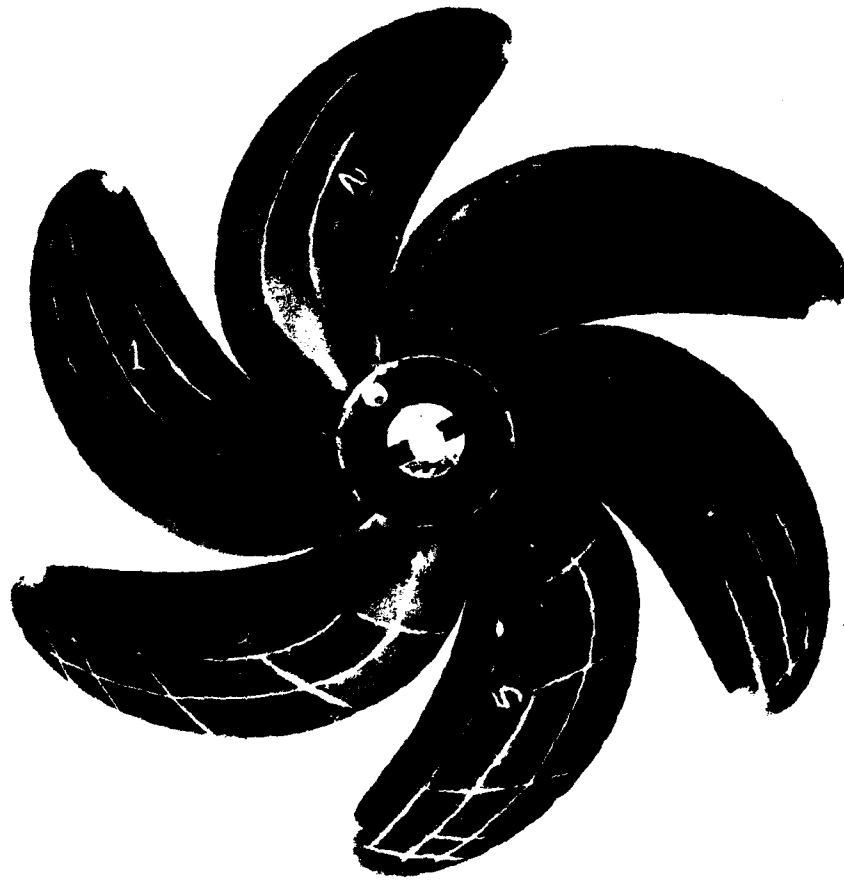
Figure 14 — Highly Skewed Model Propeller 4452

38
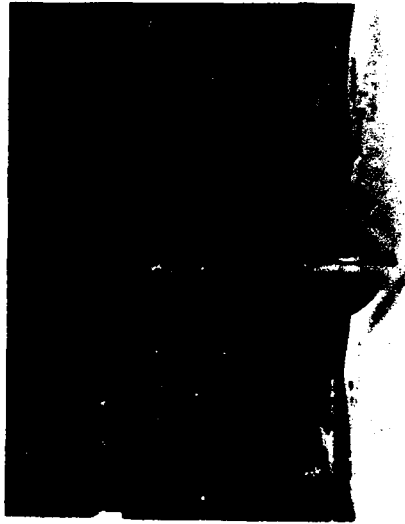
Figure 15 — Model Propeller 4452 fitted to Model Hull 5091-1

P/D

1.023
1.027
1.030
1.025
1.018
1.009
0.989
0.943
0.879

r/R
1.0
0.95
0.9
0.8
0.7
0.6
0.5
0.4
0.3
0.2

6 BLADES
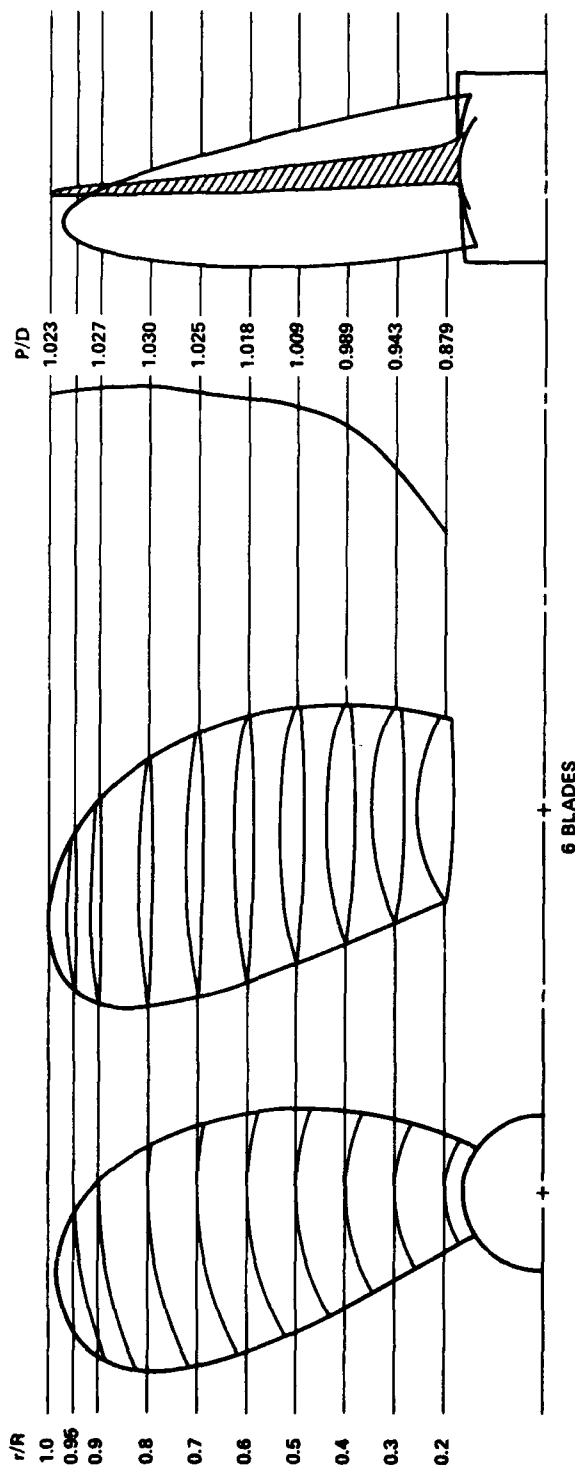
Figure 16 – Propeller Currently Fitted to Ship, Schematic
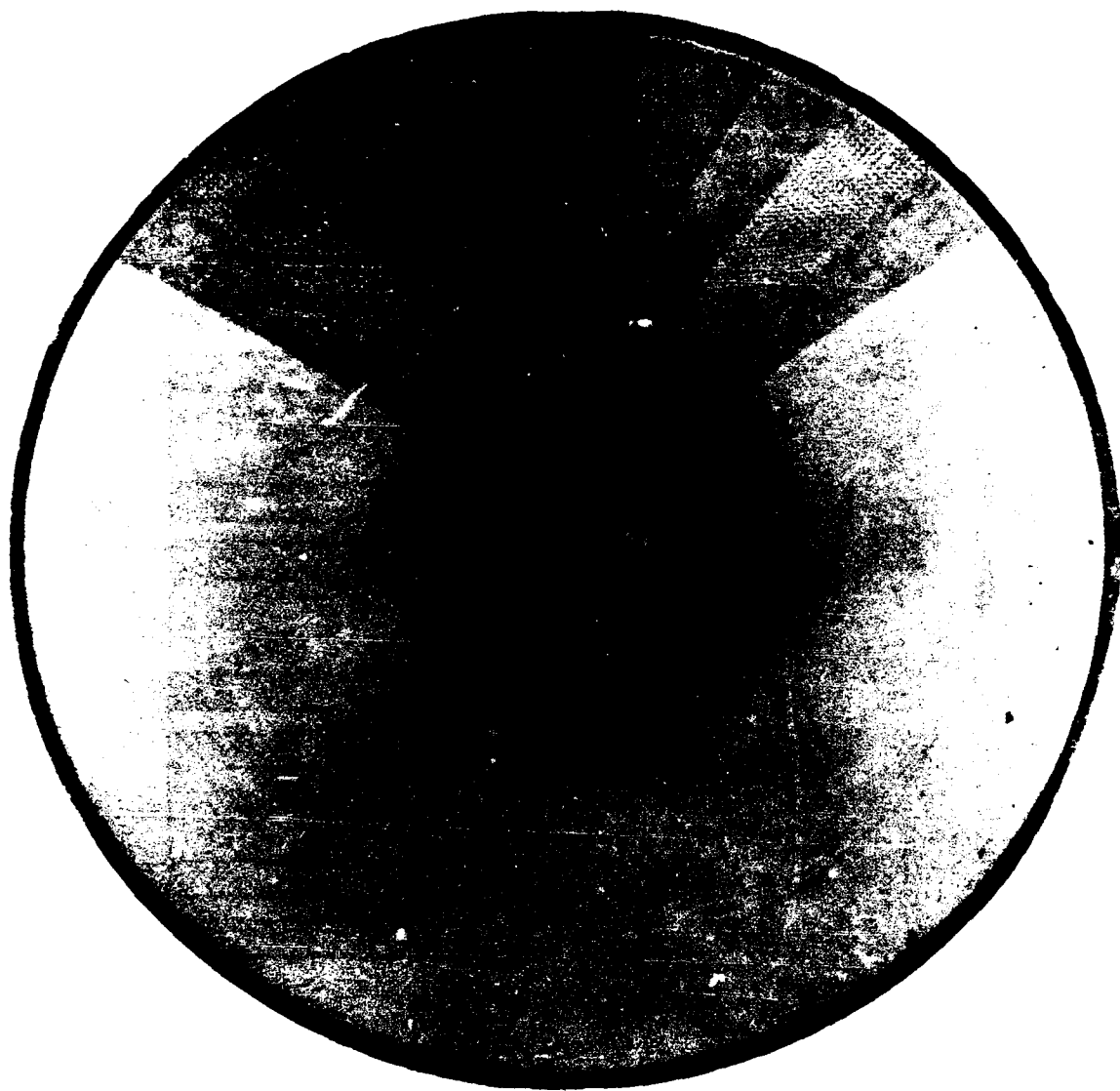
Figure 17 – Wake Screen and Highly Skewed Model Propeller 4452
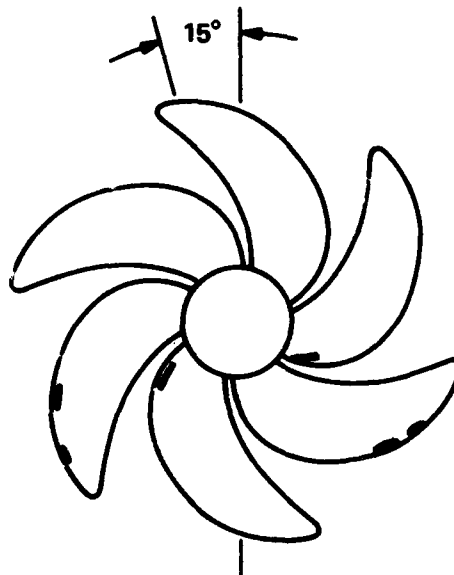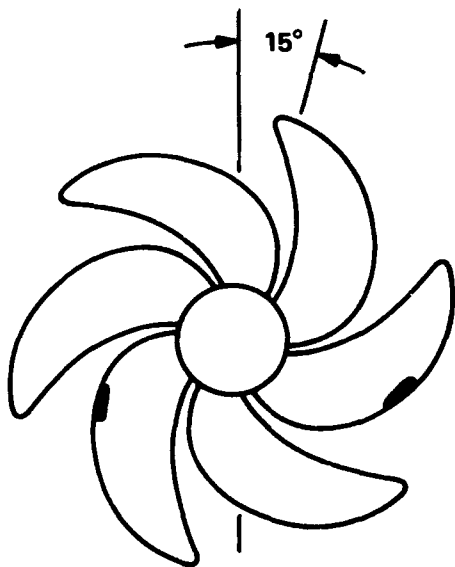
41
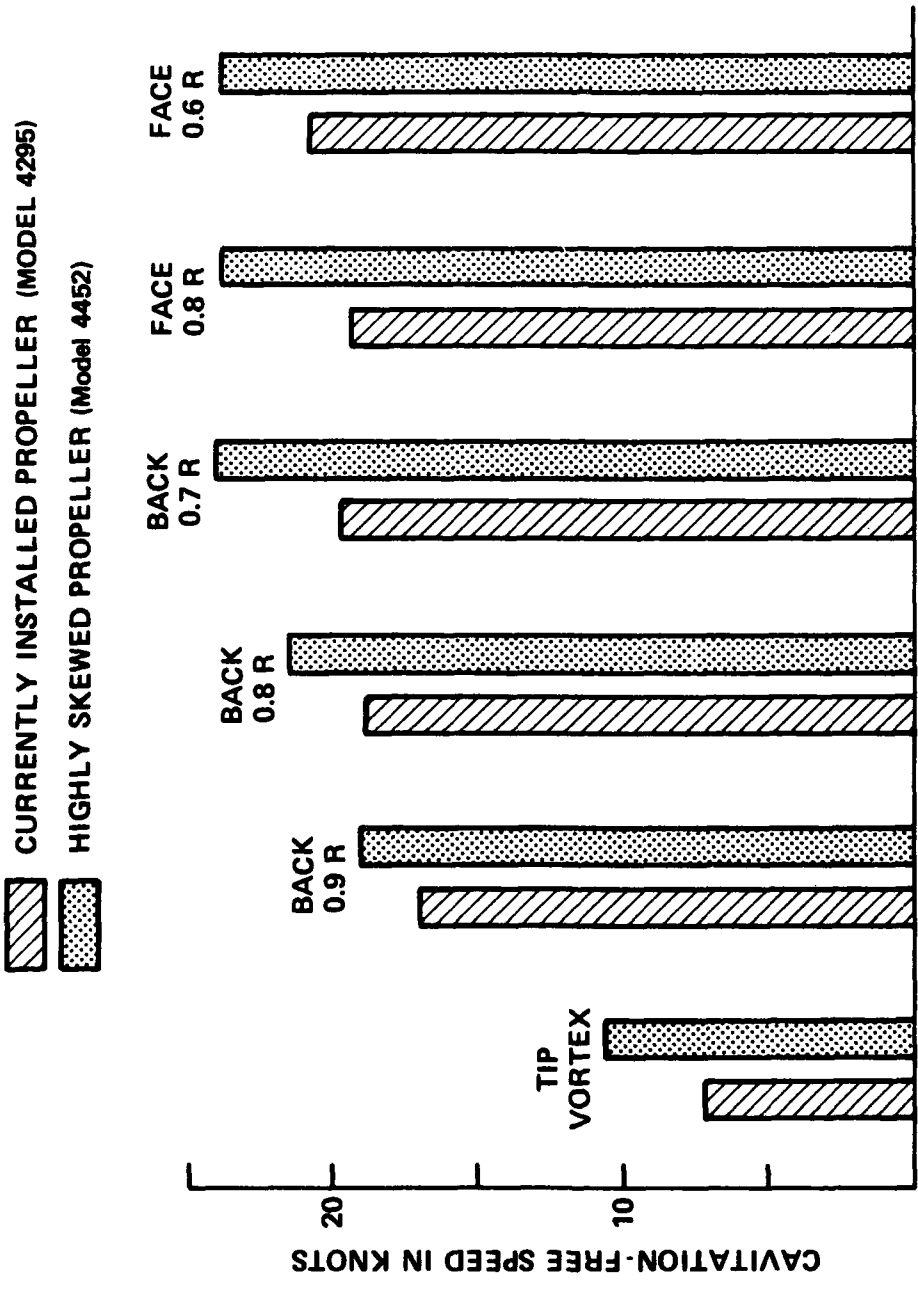
Figure 18 — Cavitation Inception at Various Radii
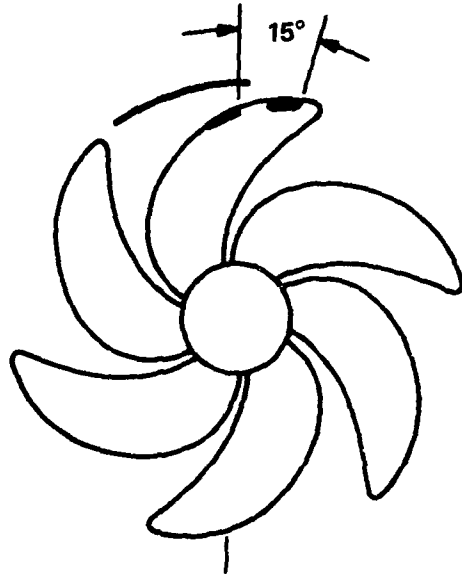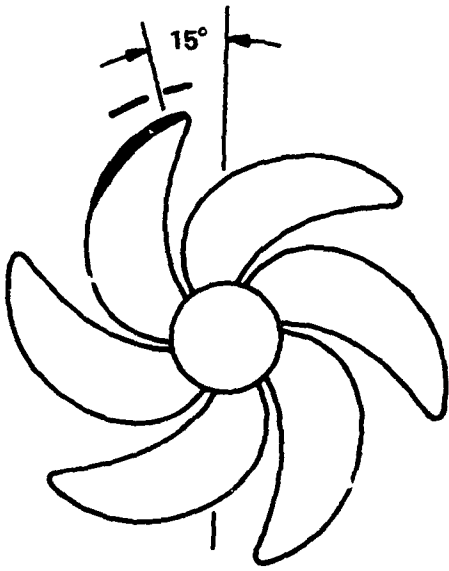
BACK
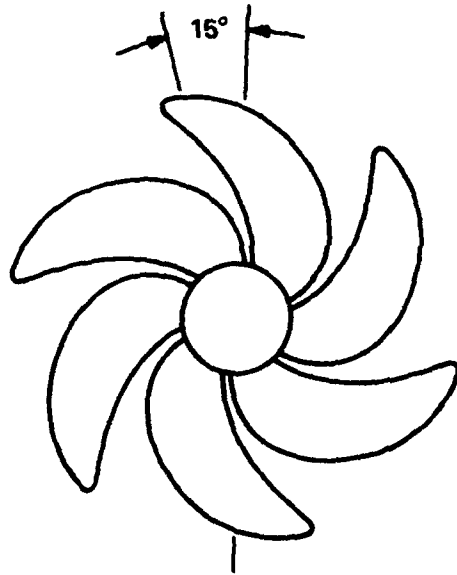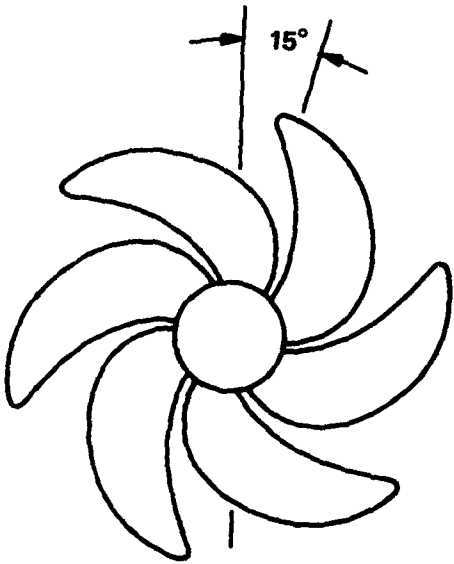
FACE

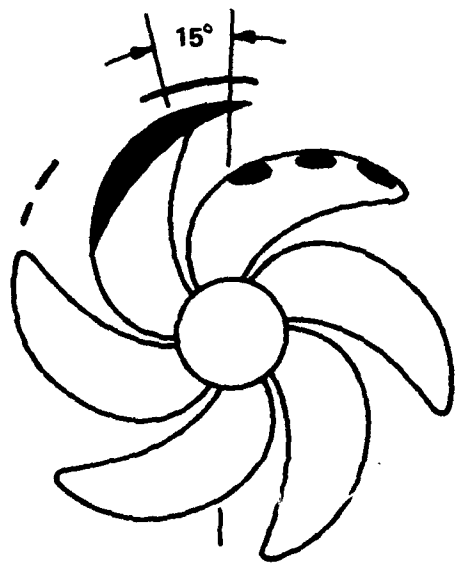Figure 19 — Cavitation at 22 Knots
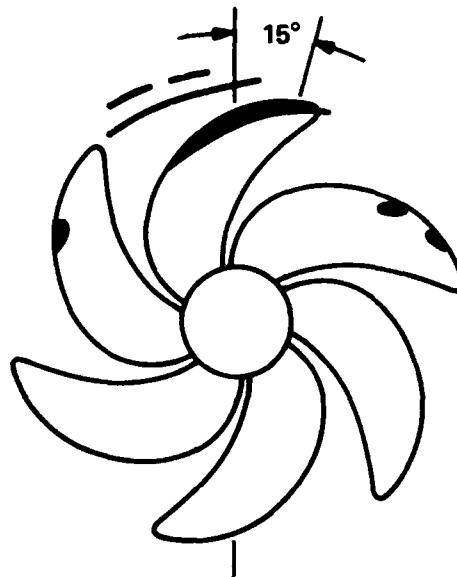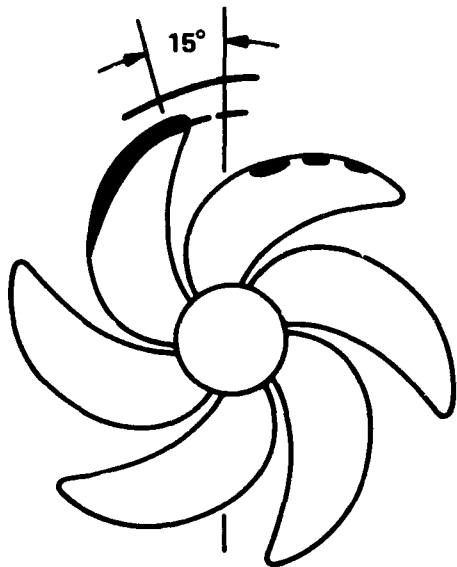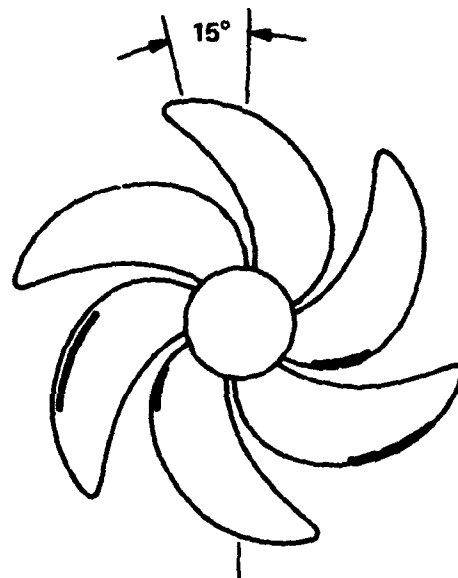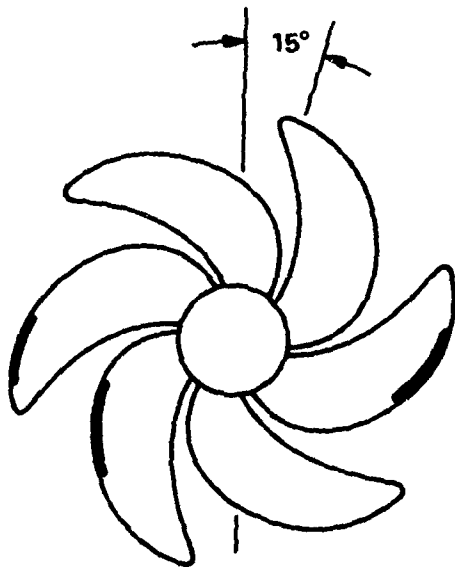
BACK

FACE

Figure 20 — Cavitation at 24.5 Knots

44
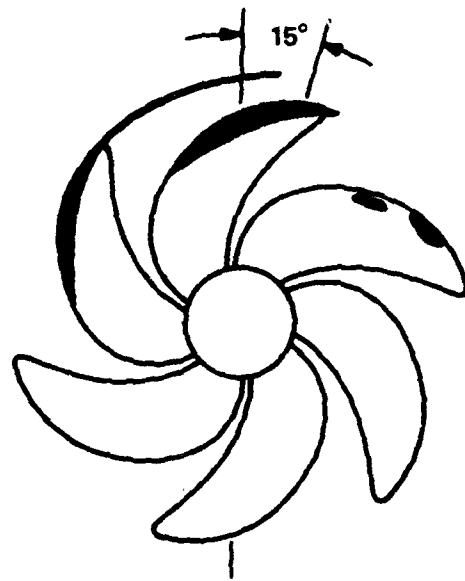
BACK

FACE

Figure 21 — Cavitation at 26 Knots
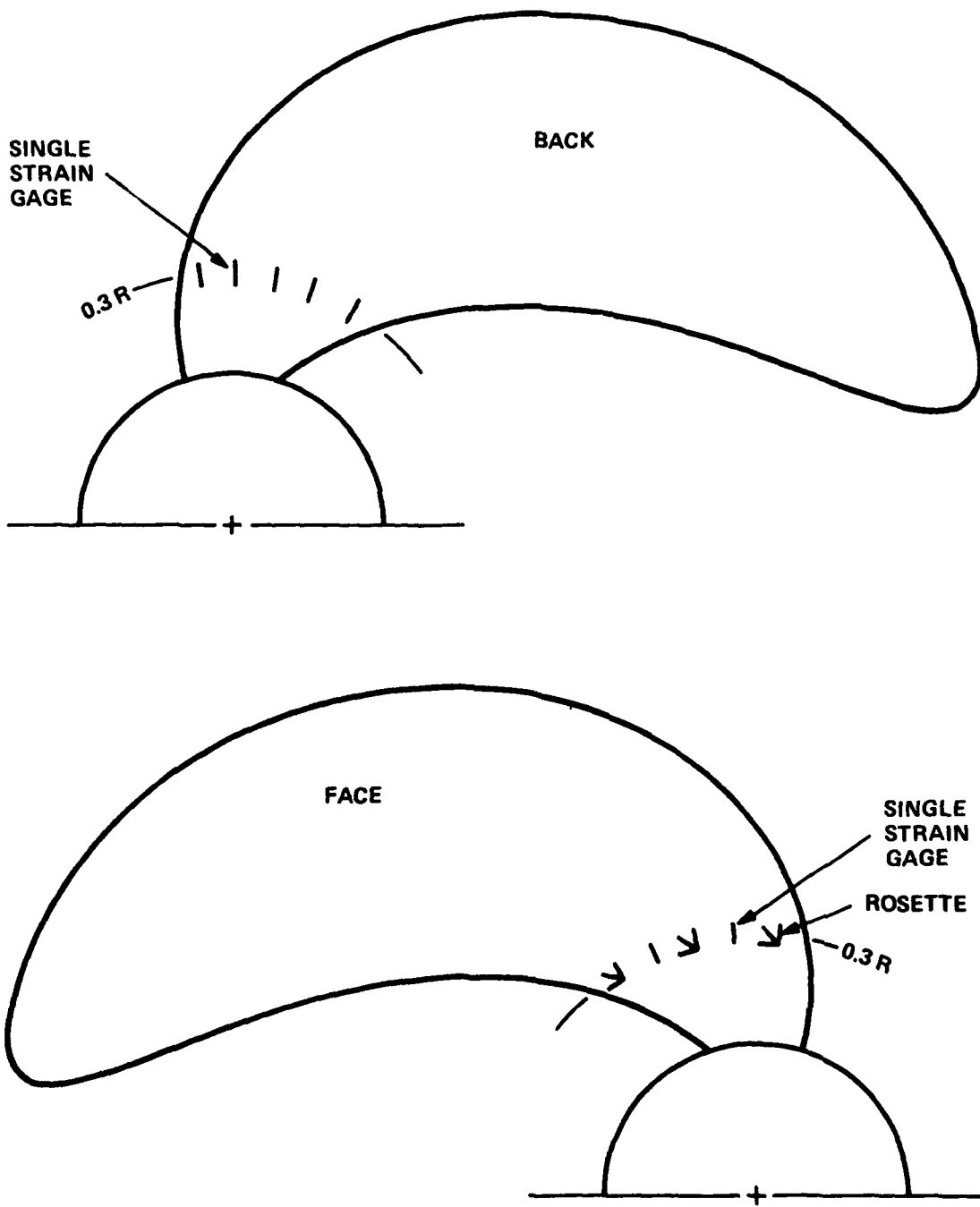
45

Figure 22 – Simulated Blade Erosion

46

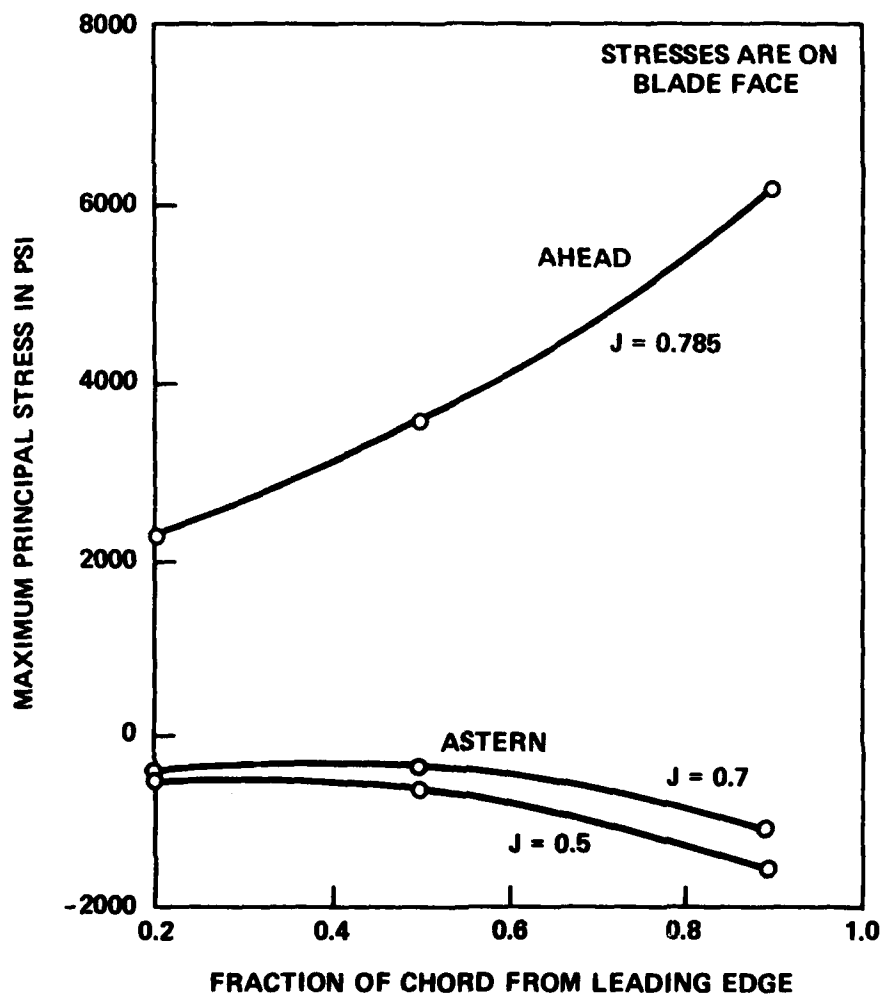Figure 23 – Location of Strain Gages and Rosettes

Figure 24 – Principal Stresses

REFERENCES

1. Cox, G.G. and W.B. Morgan, "The Use of Theory in Propeller Design," Marine Technology, Vol. 9, No. 4, pp. 419–429 (Oct 1972).

2. Cumming, R.A., W.B. Morgan, and R.J. Boswell, "Highly Skewed Propellers," Transactions of the Society of Naval Architects and Marine Engineers, Vol. 80 (1972).

3. Boswell, R.J. and M.L. Miller, "Unsteady Propeller Loading–Measurement, Correlation with Theory, and Parametric Study," NSRDC Report 2625 (Oct 1968).

4. Teel, S.S. and S.B. Denny, "Field Point Pressures in the Vicinity of a Series of Skewed Marine Propellers," NSRDC Report 3278 (Aug 1970).

5. Denny, S.B., "Cavitation and Open-Water Performance of a Series of Propellers Designed by Lifting-Surface Methods," NSRDC Report 2878 (Sep 1968).

6. Boswell, R.J., "Design, Cavitation Performance, and Open Water Performance of a Series of Research Skewed Propellers," NSRDC Report 3339 (Mar 1971).

7. Boswell, R.J., "The Effect of Skew on Cavitation of Marine Propellers," presented at the American Society of Mechanical Engineers Cavitation Forum, Pittsburgh, Pa. (Jun 1971).

8. Lerbs, H.W., "Moderately Loaded Propellers with a Finite Number of Blades and an Aribtrary Distribution of Circulation," Transactions of Society of Naval Architects and Marine Engineers, Vol. 60, pp. 73–117 (1952).

9. Morgan, W.B. and J.W. Wrench, "Some Computational Aspects of Propeller Design," Methods of Computational Physics, Vol. 4, Academic Press, Inc., New York (1965) pp. 301–331.

10. Hadler, J.B. and H.M. Cheng, "Analysis of Experimental Wake Data in Way of Propeller Plane of Single and Twin-Screw Ship Models," Transactions of Society of Naval Architects and Marine Engineers, Vol. 73, pp. 287–414 (1965).

11. Lewis, F.M., "Propeller Vibration Forces in Single Screw Ships," Transactions of Society of Naval Architects and Marine Engineers, Vol. 77, pp. 318–343 (1969).

12. Denny, S.B., "Comparisons of Experimentally Determined and Theoretically Predicted Pressures in the Vicinity of a Marine Propeller," David Taylor Model Basin Report 2349 (May 1967).

13. Van Oossanen, P. and J. van dir Kouy, "Vibratory Hull Forces Induced by Cavitating Propellers," Presented at the Spring Meeting of the Royal Institution of Naval Architects, London, England (Apr 1972).

14. Huse, E., "Pressure Fluctuations on the Hull Induced by Cavitating Propellers," Norwegian Ship Model Experimental Tank Publication 111 (Mar 1972).

15. Tsakonas, S. and W.R. Jacobs, "Propeller Loading Distributions," Journal of Ship Research, Vol. 13, No. 4, pp. 237–256 (Dec 1969).

16. Breslin, J.P., Discussion of paper, "Highly Skewed Propellers," by Cumming, Morgan, and Boswell, Transactions of Society of Naval Architects and Marine Engineers, Vol. 80 (1972).

17. Brown, N.A., Discussion of paper, "Highly Skewed Propellers," by Cumming, Morgan, and Boswell, Transactions of Society of Naval Architects and Marine Engineers, Vol. 80 (1972).

18. Burrill, L.C. and A. Emerson, "Propeller Cavitation: Further Tests on 16-Inch Model Propellers in the Kings College Cavitation Tunnel," North East Coast Institution of Engineers and Shipbuilders, Vol. 79, pp. 295–320 (1962–63).

49

19. Rader, H.P., "Cavitation Phenomena in Non-Uniform Flows," Apendix 2 of the Cavitation Committee Report, Proceedings of the 12th International Towing Tank Conference, Rome, Italy, pp. 351–364 (Sep 1969).

20. Morgan, W.B., V. Silovic, and S.B. Denny, "Propeller Lifting Surface Corrections," Transactions of Society of Naval Architects and Marine Engineers, Vol. 76, pp. 309–347 (1968).

21. Cox, G.G., "Corrections to the Camber of Constant Pitch Propellers," Transactions of the Royal Institution of Naval Architects, Vol. 103, pp. 227–243 (1961).

22. Minaas, K. and O.H. Slaattelid, "Lifting Surface Corrections for 3-Bladed Optimum Propellers," International Shipbuilding Progress, Vol. 18, No. 208, pp. 437–452 (Dec 1971).

23. Brockett, T., "Minimum Pressure Envelopes for Modified NACA Sections with NACA a = 0.8 Camber and BUSHIPS Type I and Type II Sections," David Taylor Model Basin Report 1780 (Feb 1966).

24. Van Oossanen, P., "Cavitation Testing of Marine Propellers," Schip en Werf, Vol. 39, Nos. 13 and 14 (1972); also, Netherlands Ship Model Basin Publication 418 (1972).

25. Morgan, W.B. and J.Z. Lichtman, "Cavitation Effects on Marine Devices," American Society of Mechanical Engineers, Cavitation State of Knowledge, pp. 195–241 (1969).

26. McCarthy, J.H. and J.S. Brock, "Static Stresses on Wide Bladed Propellers," Journal of Ship Research, Vol. 17, No. 2 pp. 121–134 (Jun 1970).

27. American Bureau of Shipping, "Rules for Building and Classing Steel Vessels," p. 621 (1972).

28. Cheng, H.M., "Hydrodynamic Aspect of Propeller Design Based on Lifting-Surface Theory," Parts 1 and 2, David Taylor Model Basin Reports 1802 and 1803 (Sep 1964 and Jun 1965).

29. Kerwin, J.E. and R. Leopold, "A Design Theory for Subcavitating Propellers," Transactions of Society of Naval Architects and Marine Engineers, Vol. 72, pp. 294–335 (1964).

30. Breslin, J.P., "Theoretical and Experimental Techniques for Practical Estimation of Propeller-Induced Vibratory Forces," Transactions of Society of Naval Architects and Marine Engineers, Vol. 78, pp. 23–40 (1970).

31. Lewis, F.M., "Propeller Excited Hull and Rudder Force Measurements," Massachusetts Institute of Technology, Department of Ocean Engineering Report 73-10 (Apr 1973).

32. Kerwin, J.E., "Computer Techniques for Propeller Blade Section Design," Proceedings of the Second Lips Propeller Symposium, Drunen, Holland, pp. 7–31 (May 1973).

33. Pien, P.C., Discussion of paper, "Highly Skewed Propellers," by Cumming, Morgan, and Boswell, Transactions of Society of Naval Architects and Marine Engineers, Vol. 80 (1972).

34. McCarthy, J.H., "Steady Flow Past Nonuniform Wire Grids," Journal of Fluid Mechanics, Vol. 19, Part 4 (1964).

35. McCormick, B.W., Jr., "On Cavitation Produced by a Vortex Trailing from a Lifting Surface," Journal of Basic Engineering, Vol. 84, Series D, No. 3, pp. 369–379 (Sep 1962).

36. Ito, T., "An Experimental Investigation into the Unsteady Cavitation of Marine Propellers," Ship Research Institute Paper 11, Tokyo, Japan (Mar 1966).

37. Boswell, R.J., "Static Stress Measurements on a Highly-Skewed Propeller Blade," NSRDC Report 3247 (Dec 1969).

38. Boswell, R.J. et al., "Experimental Measurements of Static Stress in a Series of Research Skewed Propellers with and without Forward Rake," NSRDC Report 3804 (in preparation).

39. Cummings, D.E., "Numerical Prediction of Propeller Characteristics," Journal of Ship Research, pp. 12–18 (Mar 1973).

40. Dhir, S.K. and J.P. Sikora, "Holographic Displacement Measurements on a Highly Skewed Propeller Blade," NSRDC Report 3680 (Aug 1971).

41. Abramson, H.N. et al., "Hydroelasticity with Special Reference to Hydrofoil Craft," NSRDC Report 2557, p. 443 (Sep 1967).

42. Bisplinghoff, R.L. et al., "Aeroelasticity," Addison-Wesley Publishing Company, Inc., Reading, Mass. (1955) p. 483.

43. Diederich,, F.W. and B. Budiansky, "Divergence of Swept Wings," National Advisory Committee for Aeronautics Technical Note 1680 (Aug 1948).